Myc stimulates B lymphocyte differentiation and amplifies calcium signaling

Tania Habib,[1] Heon Park,[1] Mark Tsang,[1] Ignacio Moreno de Alborán,[2] Andrea Nicks,[1] Leslie Wilson,[1] Paul S. Knoepfler,[4] Sarah Andrews,[3] David J. Rawlings,[3] Robert N. Eisenman,[4] and Brian M. Iritani[1,4]

[1]Department of Comparative Medicine, University of Washington, Seattle, WA 98195
[2]Department of Immunology and Oncology, Centro Nacional de Biotecnología, Universidad Autonoma de Madrid, Cantoblanco, Madrid 28049, Spain
[3]Immunology Clinic, Children's Hospital and Regional Medical Center, Seattle, WA 98104
[4]Division of Basic Sciences, Fred Hutchinson Cancer Research Center, Seattle, WA 98109

Deregulated expression of the Myc family of transcription factors (c-, N-, and L-*myc*) contributes to the development of many cancers by a mechanism believed to involve the stimulation of cell proliferation and inhibition of differentiation. However, using B cell–specific c-/N-*myc* double-knockout mice and Eμ-*myc* transgenic mice bred onto genetic backgrounds (recombinase-activating gene $2^{-/-}$ and $Btk^{-/-}$ $Tec^{-/-}$) whereby B cell development is arrested, we show that Myc is necessary to stimulate both proliferation and differentiation in primary B cells. Moreover, Myc expression results in sustained increases in intracellular Ca^{2+} ($[Ca^{2+}]_i$), which is required for Myc to stimulate B cell proliferation and differentiation. The increase in $[Ca^{2+}]_i$ correlates with constitutive nuclear factor of activated T cells (NFAT) nuclear translocation, reduced Ca^{2+} efflux, and decreased expression of the plasma membrane Ca^{2+}–adenosine triphosphatase (PMCA) efflux pump. Our findings demonstrate a revised model whereby Myc promotes both proliferation and differentiation, in part by a remarkable mechanism whereby Myc amplifies Ca^{2+} signals, thereby enabling the concurrent expression of Myc- and Ca^{2+}-regulated target genes.

Introduction

Members of the Myc family of nuclear protooncogenes are known to stimulate cell division and transformation. However, the roles of Myc in cell differentiation have been difficult to assess, in part because of the early embryonic lethality of N-*myc*– (Charron et al., 1992) and c-*myc* (Davis et al., 1993)–null mice and the difficulties in experimentally distinguishing proliferation from differentiation using in vitro approaches. In this study, we used B cell–specific deletion or overexpression of c- and/or N-*myc* to explore the roles of Myc in B lymphocyte development and lymphoma formation. B cell development in the bone marrow (BM) and fetal liver are marked by a series of cell fate decisions, which are controlled by checkpoints that ensure that all mature B lymphocytes are capable of producing functional antibodies (for review see Hendriks and Middendorp, 2004). Pluripotent hematopoietic progenitors initially become committed to the B lineage in response to growth factors and stromal cell interactions. The least mature committed B cell progenitors, called pro–B cells, have their Ig heavy chain (HC) and light chain (LC) genes in germline (GL) configuration. The Ig HC genes rearrange before the Ig LCs, and with successful in-frame D_H-J_H and then V_H-D_H-J_H juxtaposition, the Ig HCμ appears at the cell surface along with the signal-transducing proteins Igα and Igβ and the surrogate LC λ5 and Vpre-B1 and 2 as a complex called the pre–B cell receptor (BCR; termed large pre–B cells). The pre-BCR then signals large pre–B cells to proliferate, mature to the small pre–B cell stage, extinguish rearrangement of the other allele of the Ig HC (a process called allelic exclusion), and initiate Ig LC transcription and rearrangement (Vκ and Vλ). Successful in-frame Ig V_L-J_L rearrangement allows the Ig HC and LC proteins to pair and form IgM molecules on the surface of immature B cells, at which point they migrate from the BM to the periphery, where development continues.

Formation of the pre-BCR represents a critical checkpoint for ensuring that maturing B cells have in-frame V_H-D_H-J_H gene rearrangements. Signaling is induced by pre-BCR aggregation in lipid rafts, resulting in activation of the Src family protein

Correspondence to Brian M. Iritani: biritani@u.washington.edu

Abbreviations used in this paper: BCR, B cell receptor; BM, bone marrow; CFA, complete Freund's adjuvant; CFSE, 5-carboxyfluorescein diacetate succinimidyl ester; ChIP, chromatin immunoprecipitation; Cn, calcineurin; CsA, cyclosporine A; GL, germline; HC, heavy chain; HSA, heat-stable antigen; IRES, internal ribosomal entry site; KLH, keyhole limpet hemocyanin; LC, light chain; MSCV, murine stem cell virus; MZ, marginal zone; NFAT, nuclear factor of activated T cells; NF-κB, nuclear factor κB; PE, phycoerythrin; PI3K, phosphatidylinositol 3-kinase; PMCA, plasma membrane Ca^{2+}-ATPase; PTK, protein tyrosine kinase; qPCR, quantitative PCR; RAG2, recombinase-activating gene 2; SERCA, sarcoplasmic ER Ca^{2+} ATPase; Tg, transgene; Wt, wild type.

The online version of this article contains supplemental material.

The Journal of Cell Biology, Vol. 179, No. 4, November 19, 2007 717–731
http://www.jcb.org/cgi/doi/10.1083/jcb.200704173

tyrosine kinases (PTKs) Blk, Lyn, and Fyn, which then phosphorylate tyrosine residues within Igα and Igβ. This results in recruitment and activation of the Syk PTK (and to a lesser extent ZAP70) and the adaptor SLP-65 (also known as BASH or BLNK). Phosphorylation of SLP-65 by Syk further activates multiple signaling pathways, including the Ras–Raf and phosphatidylinositol 3-kinase (PI3K) pathways, as well as the Tec family PTKs Btk and Tec, which, together with Syk, activate PLCγ, resulting in Ca^{2+} mobilization (see Fig. 8; for review see Hendriks and Middendorp, 2004). Altogether, these events result in expression and/or activation of a set of transcription factors including extracellular regulated kinase, nuclear factor of activated T cells (NFAT), nuclear factor κB (NF-κB), and Myc.

Targeted deletion studies in mice have revealed essential roles for the majority of the described surface and cytoplasmic molecules in the development of pre–B cells (for review see Hendriks and Middendorp, 2004). However, the roles of nuclear factors such as Myc in B cell development remain unclear, in part because of genetic redundancy by related transcription family members or lethality after tissue-wide deletion. The Myc family of basic helix-loop-helix transcription factors bind DNA sequences called E boxes (CACGTG) as a heterodimer with the related basic helix-loop-helix factor Max (for review see Eisenman, 2001). This results in initiation of transcription, although transcriptional repression by Myc has been noted, probably through inhibition of the Miz-1 transcription factor (Li et al., 1994; Staller et al., 2001). Of the three mammalian *myc* family members, only c- and N-*myc* are expressed in B lymphocytes. c-*myc* is initially expressed during the pro–B cell stage in response to cytokines, including IL-7 (Morrow et al., 1992; Dillon and Schlissel, 2002). After pre-BCR expression in large pre–B cells, both c- and N-*myc* are expressed during the maturation and expansion to small pre–B cells (Zimmerman and Alt, 1990). Thereafter, only c-*myc* is expressed in immature and mature B cells after B cell activation. In this study, we took a unique genetic approach in mice to show that Myc stimulates B cell differentiation and expansion downstream of the pre-BCR and Tec PTKs. Moreover, we uncover a novel feature of Myc in amplifying $[Ca^{2+}]_i$ as a mechanism to concurrently stimulate the expression of both Myc and Ca^{2+}-regulated genes, which are essential for both cell division and differentiation.

Results

Mice deficient in Myc have impaired pre–B cell development

To examine the roles of Myc in early B cell development and to overcome potential functional redundancy between c- and N-*myc*, we generated mice deficient in both N- and c-*myc* genes selectively in B cells using the Cre-loxP system (Sauer, 2002). c-$myc^{fl/fl}$ mice (de Alboran et al., 2001) were bred to N-$myc^{fl/fl}$ mice (Knoepfler et al., 2002), which also carried the CD19*cre* transgene (Tg), to generate N-$myc^{fl/fl}$ c-$myc^{fl/fl}$ $CD19cre^+$ mice. The CD19 promoter drives expression of the Cre recombinase only in B lineage cells throughout their development (Rickert et al., 1997). Semi-quantitative PCR (qPCR) analysis of sorted $B220^+CD43^+$ and $B220^+CD43^-$ B cell progenitors in the BM revealed ∼75/90% deletion of c-*myc* and ∼70/95% deletion of N-*myc* genes, respectively, in the presence of CD19cre (Fig. S1 A, available at http://www.jcb.org/cgi/content/full/jcb.200704173/DC1).

Total BM cells were isolated from mice deficient in c- and/or N-*myc* selectively in B cells, and B cell development was analyzed using flow cytometry (see Fig. 3 A; Hardy and Hayakawa, 2001). Decreasing c-*myc* expression alone (c-$myc^{fl/fl}$ $CD19cre^+$) impairs the generation of $B220^+CD43^-$ pre–B cells, whereas decreasing N-*myc* expression alone (N-$myc^{fl/fl}$ $CD19cre^+$) does not consistently have any effect (unpublished data). However, depletion of total *myc* expression in N-$myc^{fl/fl}$ c-$myc^{fl/fl}$ $CD19cre^+$ mice results in maximal decreases in the percentage (Fig. 1 A) and number (Fig. 1 B) of $B220^+CD43^-$, $B220^+IA^{b+}$ pre–B cells, immature B cells ($B220^{lo}IgM^+$), and mature B cells ($B220^{hi}IgM^+$) relative to $CD19cre^-$ mice. These results suggest that Myc is required for pro–B to pre–B cell maturation.

In mice, pre–B cells proliferate in response to cytokines such as IL-7 produced by BM stromal cells (Fleming and Paige, 2002). Because IL-7 signaling is known to stimulate the expression of c-*myc*, we examined the ability of B cell progenitors to divide in response to IL-7. Total BM cells from N-$myc^{fl/fl}$ c-$myc^{fl/fl}$ $CD19cre^+$ or $CD19cre^-$ mice were labeled with 5-carboxyfluorescein diacetate succinimidyl ester (CFSE) and cultured in the presence or absence of IL-7 for 36 h, and the cell division profile of B cell progenitors was examined. As shown in Fig. 1 C, the majority of B cell progenitors from either N-$myc^{fl/fl}$ c-$myc^{fl/fl}$ $CD19cre^-$ or $CD19cre^+$ mice do not divide in the absence of IL-7. However, in response to IL-7, pre–B cells from $CD19cre^-$ mice undergo an average of four divisions, whereas cells from $CD19cre^+$ mice either do not divide at all or undergo several divisions, likely as a result of the loss of cells that contain the deleted c-*myc* alleles (Fig. S1 B; de Alboran et al., 2001).

To determine whether the reduction in *myc* levels affects the development of peripheral B cells, we purified splenocytes from N-$myc^{fl/fl}$ c-$myc^{fl/fl}$ $CD19cre^+$ and $CD19cre^-$ mice and characterized B cell subsets by flow cytometry. Splenic B cells are subdivided into additional stages of maturation and function, including transitional 1 and 2 (T1 and T2), follicular mature, and marginal zone (MZ; Hardy and Hayakawa, 2001). As shown in Fig. 2 A, $CD19cre^+$ mice exhibit a significant reduction in the number of all B cell subsets. This correlates with reduced serum IgM, IgG2a, and IgG1 in $CD19cre^+$ compared with $CD19cre^-$ mice after immunization with keyhole limpet hemocyanin (KLH; Fig. 2 C). These results suggest that Myc regulates final B cell numbers in part by regulating pre–B cell development and, potentially, peripheral B cell differentiation.

Peripheral B cells can be further classified as B2 conventional B cells, which reside in lymphoid tissues such as the spleen, and as B1 B cells, which represent the majority of B cells found in peritoneal and pleural cavities and are IgM^{hi}, $CD5^{+/-}$, and $CD23^-$. As shown in Fig. 2 B, deletion of c- and N-*myc* together results in a decrease in both $CD5^{lo}IgM^{hi}$ peritoneal B1 B cells and $CD5^-IgM^{hi}$ B2 B cells. These results suggest that

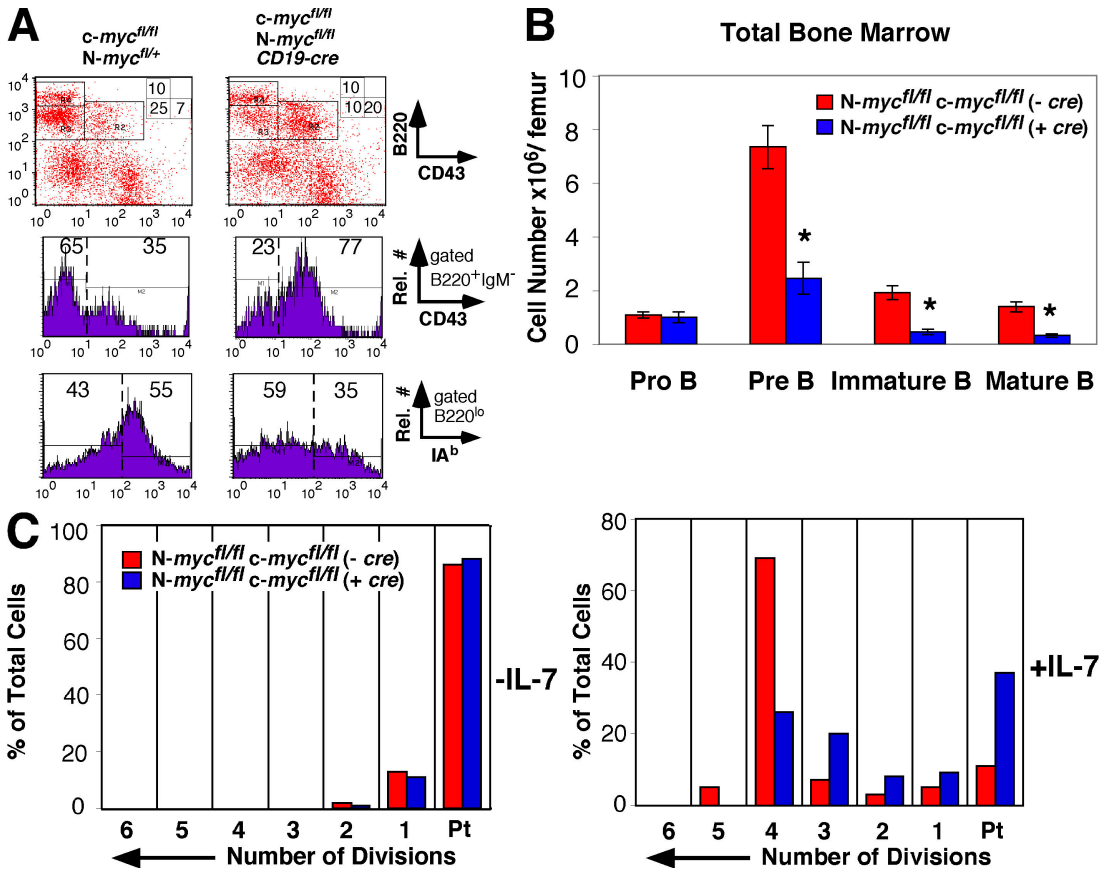

Figure 1. **Deletion of c-and N-*myc* in B lineage cells results in impaired pre–B cell development.** (A) Deletion of c-and N-*myc* in B lineage cells leads to a reduction in the pre–B, immature B, and mature B cell compartments in the BM. Flow cytometric analysis of BM cells stained with αB220, αCD43, αIgM, and αIA^b. Numbers indicate the percentage of cells in each region. (B) Total BM cells were stained with αB220, αCD43, and αIgM and analyzed by flow cytometry. Relative numbers of each population were determined as described in Materials and methods. Bars represent the mean ± SEM (error bars) obtained from three CD19*cre*$^-$ and four CD19*cre*$^+$ animals. *, $P < 0.005$. (C) Deletion of c-and N-*myc* results in impaired pre–B cell proliferation. BM cells from mice of the indicated genotypes were labeled with CFSE and cultured in the absence (left) or presence (right) of IL-7 for 36 h. Cultures were stained with αB220 and αCD43 and analyzed by flow cytometry. Panels represent the number of B220$^+$CD43$^-$ cell divisions after MODFIT analysis of CFSE histograms. Bars represent the percentage of total cells in each generation relative to parental (Pt) cells. Results are representative of four separate experiments.

Myc is essential for the development of both B2 and B1 B cells and for establishing final B cell numbers.

Eμ-*myc* Tg stimulates the maturation and expansion of RAG2-null pro-B cells

It is unclear from the gene-targeting strategy whether the effects of Myc are exclusively in modulating the expansion of a population of cells that have already differentiated to the pre–B cell stage or whether Myc may also stimulate the differentiation of pre-BCR$^+$ cells. To address this question, we took a classical genetic approach to determine whether Myc could rescue B cell differentiation in the absence of upstream signaling molecules known to be required for both *myc* expression and pre–B cell differentiation. In pre–B cells, *myc* genes are expressed, in part, by a pathway involving pre-BCR formation; the activation of Tec kinases, PLCγ, and PKC; and NF-κB translocation to the *myc* promoter (see Fig. 8; Grumont et al., 2002). First, we determined whether Myc could rescue B cell differentiation in the absence of pre-BCR formation by breeding Eμ-*myc* transgenic mice (Harris et al., 1988), which express c-*myc* exclusively in B lineage cells throughout development, to mice deficient in recombinase-activating gene 2 (RAG2; Shinkai et al., 1992), a gene required for the initiation of V(D)J recombination. RAG2$^{-/-}$ mice lack pre-BCR expression, resulting in a complete block in B cell development at the B220$^+$CD43$^+$CD25$^-$ pro–B cell stage (Fig. 3 A, Hardy fraction C). We find that c-*myc* Tg is sufficient to stimulate the differentiation of RAG2-deficient pro–B cells based on the acquisition of pre–B cell characteristics, including the down-regulation of CD43 and the up-regulation of CD25, IA^b, CD22, and heat-stable antigen (HSA; Fig. 3, A–C). This translates to a rescue in the relative number of pre–B-like cells to a level equivalent to that of wild-type (Wt) mice based on an increase in the number and ratio of B220$^+$CD43$^-$ cells to B220$^+$CD43$^+$ cells in BM from Eμ-*myc*/RAG2$^{-/-}$ as compared with RAG2$^{-/-}$ mice (unpublished data). c-Myc also stimulates GL transcription of the Igκ LC in purified B cell progenitors from Eμ-*myc*/RAG2$^{-/-}$ as compared with RAG2$^{-/-}$ mice (Fig. 3, A and D). Myc does not appear to induce allelic exclusion of the Ig HC (Fig. S2 C, available at http://www.jcb.org/cgi/content/full/jcb.200704173/DC1), suggesting that Myc Tg is not sufficient to mediate all of the signals from the pre-BCR.

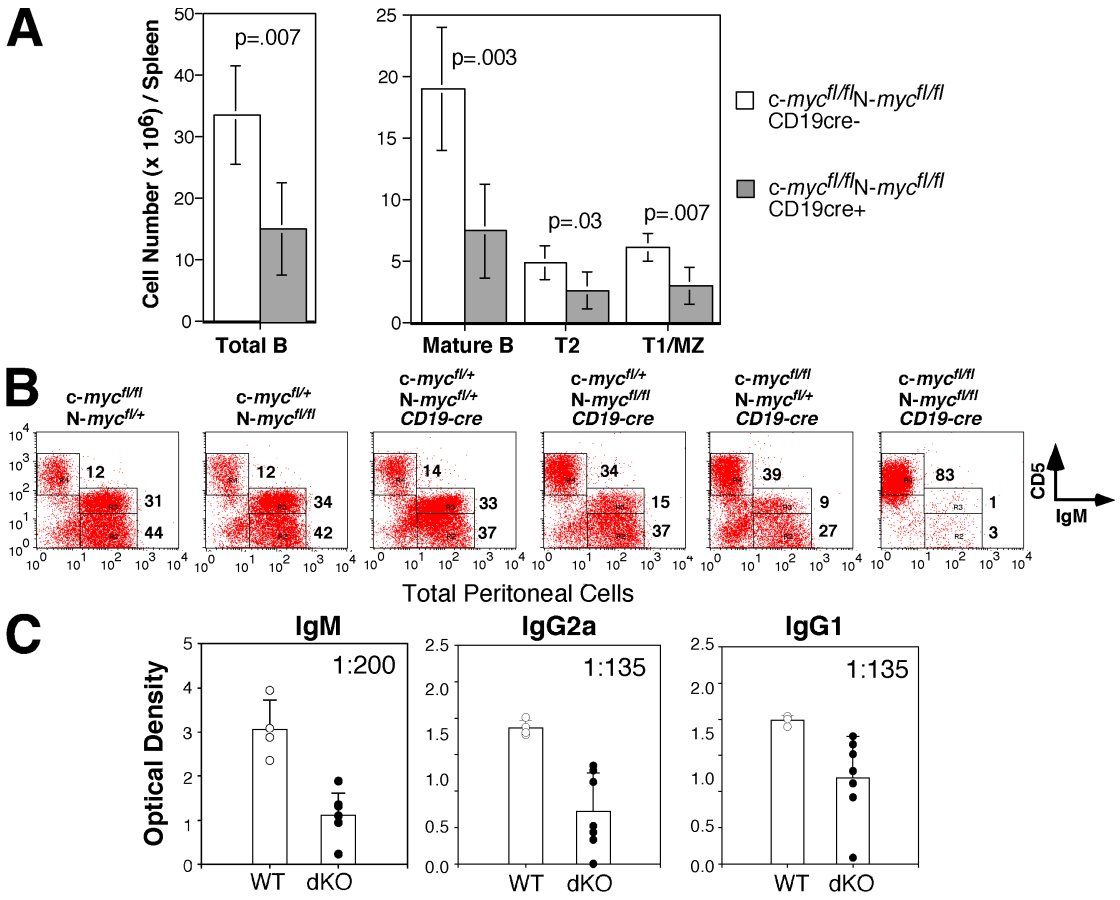

Figure 2. **Deletion of c- and N-*myc* results in impaired B1 and B2 B cell development.** (A) Splenic B cells from mice of the indicated genotypes (10–11 wk) were stained with antibodies to B220, IgM, and IgD. Relative numbers of total B cells ($B220^+IgM^+$), follicular mature ($IgM^{lo}IgD^{hi}$), T2 ($IgM^{hi}IgD^{hi}$), and T1/MZ ($IgM^{hi}IgD^{lo}$) B cells were determined as described in Materials and methods. Bars represent the mean ± SEM (error bars) obtained from six CD19*cre*$^-$ and four CD19*cre*$^+$ mice. (B) Impaired B1 cell development in c-/N-*myc*–deficient mice. Peritoneal cells were stained with antibodies to B220, IgM, and CD5 and analyzed by flow cytometry. Numbers in dot plots indicate the percentage of $CD5^+IgM^-$, $CD5^{lo}IgM^{hi}$ (B1 B), and $CD5^-IgM^{hi}$ (B2 B) populations. Data are representative of three separate experiments. (C) Decreased antibody production in *myc*-deficient mice. Mice were immunized with KLH-CFA, and the KLH-specific serum antibody concentrations were determined by ELISA. Bars represent the mean ± SEM of four Wt and seven CD19*cre*$^+$ c-*myc*$^{fl/fl}$ N-*myc*$^{fl/fl}$ mice. Serum dilutions are shown. dKO, double knockout.

To further examine the proliferative capacity of Eμ-*myc*/$RAG2^{-/-}$ versus $RAG2^{-/-}$ B cell progenitors, we labeled BM cells with BrdU, which is incorporated into DNA during cell division, and with CFSE. The percentage of $B220^+BrdU^+$ cells is higher in Eμ-*myc*/$RAG2^{-/-}$ compared with $RAG2^{-/-}$ mice (Fig. S2 A), and B cells from Eμ-*myc*/$RAG2^{-/-}$ mice undergo considerably more cell divisions than B cells from $RAG2^{-/-}$ mice in response to IL-7 stimulation (Fig. 3 E). In contrast, we do not see any difference in the number of apoptotic $B220^+$ cells between Eμ-*myc*/$RAG2^{-/-}$ compared with $RAG2^{-/-}$ mice based on the acquisition of the apoptotic marker annexin V (Fig. S2 B).

Eμ-*myc* Tg rescues B cell maturation in mice deficient in Btk and Tec kinases

To further characterize the upstream signaling pathway involved in Myc-dependent differentiation, we determined whether Myc could rescue B cell differentiation in the absence of the Tec family PTKs, which mediate proliferation and differentiation downstream of the pre-BCR and BCR (see Fig. 8). We bred Eμ-*myc* mice to mice doubly deficient in expression of the Tec family PTKs Btk and Tec (Ellmeier et al., 2000). In humans, loss of function mutations in the *btk* gene lead to X-linked agammaglobulinemia, an immunological disease whereby Ca^{2+} signaling is impaired (Fluckiger et al., 1998; for review see Rawlings, 1999) and the generation of pre–B cells is blocked. In mice, pre–B cell development is only partially inhibited in *btk*-deficient mice and proceeds normally in *tec*-deficient mice but is essentially completely inhibited in *btk/tec* double-null mice. Thus, we asked whether Myc could rescue B cell development when Tec family signaling is ablated. As shown in Fig. 4 A, $btk^{-/-}tec^{-/-}$ mice are deficient in their ability to generate pre–B cells based on a reduction in $B220^+CD43^-$ B cell progenitors compared with Wt mice. However, when c-*myc* is expressed in $btk^{-/-}tec^{-/-}$ B cell progenitors, both the percentage (Fig. 4 A) and total number (not depicted) of $B220^+CD43^-$, $B220^+CD22^+$, and $B220^+IA^{b+}$ pre–B cells and $B220^+IgM^+$ immature B cells are completely rescued. These results provide additional genetic evidence that Myc stimulates B cell development downstream of the pre-BCR and Tec family PTKs.

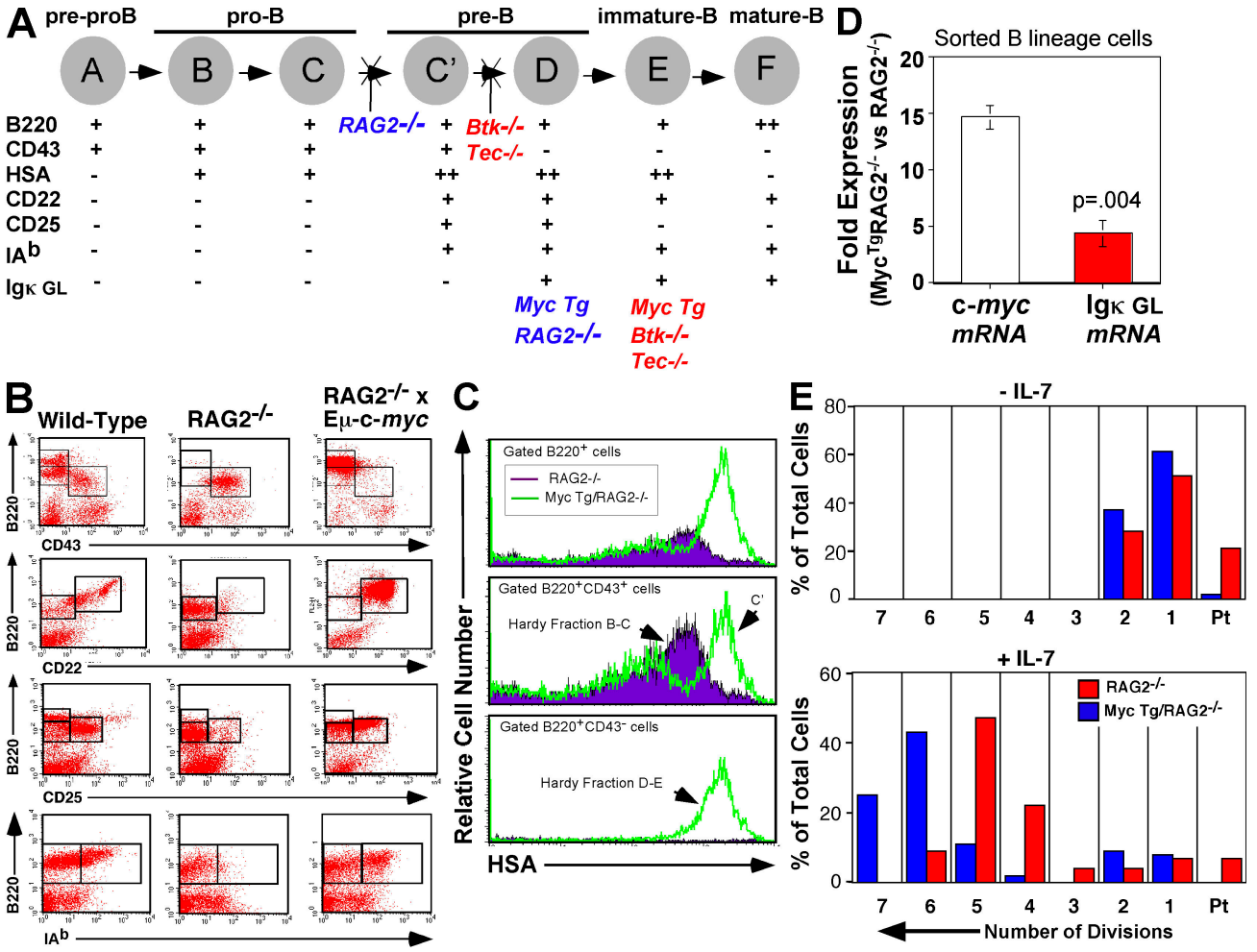

Figure 3. **c-Myc stimulates B cell development, proliferation, and GL Igκ transcription in RAG2-null mice.** (A) A model of B cell development based on the expression of B220, CD43, HSA, CD22, CD25, IA^b, and Igκ (modified from Hardy and Hayakawa, 2001). (B) c-Myc stimulates pre–B cell–like differentiation in RAG2-null mice. BM cells were stained with αB220, αCD43, αCD22, αCD25, and αIA^b. Representative flow dot plots (of 10 experiments) corresponding to mice of the indicated genotypes are shown. (C) BM cells from $RAG2^{-/-}$ or Eμ-*myc*/$RAG2^{-/-}$ mice were stained for the expression of B220, CD43, and HSA. Representative histogram overlays of HSA expression on gated $B220^+$ cells (top), $B220^+CD43^+$ cells (middle), or $B220^+CD43^-$ cells (bottom) are shown. (D) Real-time qPCR analysis of c-*myc* and Igκ GL message from FACS-sorted $B220^+$ Eμ-*myc*/$RAG2^{-/-}$ and $RAG2^{-/-}$ B cell progenitors. The fold expression ratio (Myc$RAG2^{-/-}$/$RAG2^{-/-}$) of c-*myc* and Igκ GL mRNA is shown. Bars represent the mean ratio ± SEM (error bars). (E) Eμ-*myc*/$RAG2^{-/-}$ $B220^+$ B cell progenitors exhibit increased proliferative capacity compared with $RAG2^{-/-}$ B cells as assessed by CFSE dilution after 72-h culture in IL-7 as described in Fig. 1 C. Results are representative of three separate experiments.

Loss of Btk and Tec increases the tumor frequency in Eμ-*myc* transgenic mice

Because Tec kinases have been reported to both induce and suppress tumor formation (Hendriks and Kersseboom, 2005), we investigated how the transformation capacity of Eμ-*myc* Tg is altered by the loss of Btk and Tec. We find that the heterozygosity of *btk* and *tec* is sufficient to increase the tumor frequency in Eμ-*myc* mice, with the 50% tumor incidence being reduced from 100 d for Eμ-*myc* mice to 60 d for Eμ-*myc*/$btk^{-/+}$ $tec^{-/+}$ (Fig. 4 B). The percent tumor-free incidence was decreased further as additional alleles of *btk* or *tec* were deleted. These results suggest that deregulated c-*myc* synergizes with the loss of Tec signaling during B cell lymphoma formation. Interestingly, ∼75% of the tumors that develop in Eμ-*myc*/$btk^{-/-}tec^{-/+}$ or Eμ-*myc*/$btk^{-/-}tec^{-/-}$ mice express surface IgM (unpublished data), indicating that they have an immature B cell phenotype relative to the majority of tumors derived from Eμ-*myc* Tg mice, of which >80% are IgM^- pre–B cell tumors (Harris et al., 1988).

c-Myc–expressing B cells exhibit elevated Ca^{2+} levels and NFAT nuclear translocation

Ca^{2+} signaling is induced by the pre-BCR and is modulated by Btk (for review see Rawlings, 1999), and, in T lymphocytes (Aifantis et al., 2001) as well as in many other cell types, is required for the induction of differentiation. Because Myc rescues B cell differentiation in the absence of the pre-BCR and Btk, we investigated whether Myc can bypass requirements for normal Ca^{2+} signaling or whether Myc amplifies Ca^{2+} signaling in the absence of the pre-BCR or Btk. In B cells, the sustained Ca^{2+} flux after BCR cross-linking is thought to be caused by the concurrent activation of PI3K, which leads to the production of membrane-associated PI-3,4,5-P3 and to the recruitment and phosphorylation of Btk. Btk activation results in full and

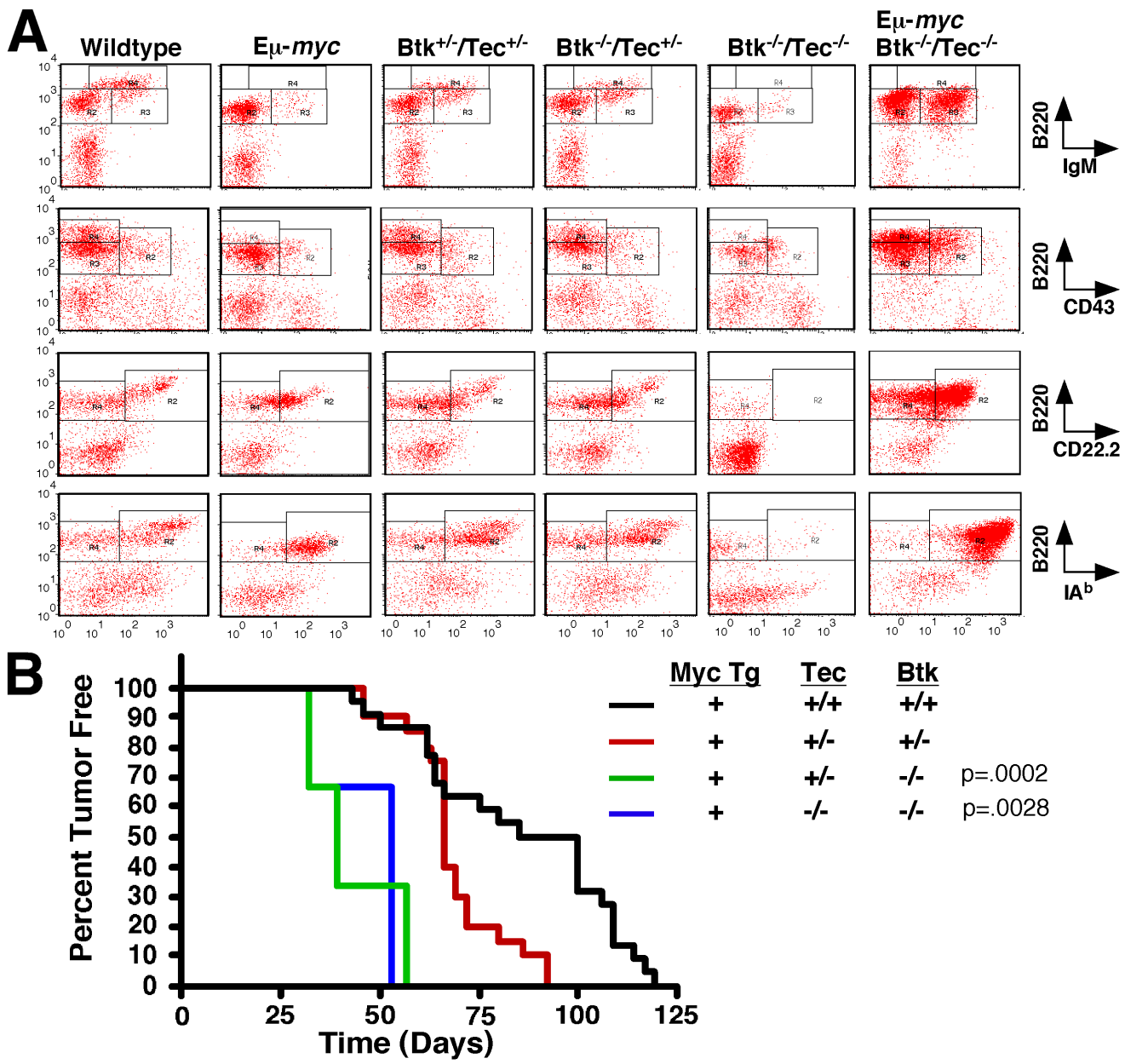

Figure 4. **Increased B cell maturation and tumor frequency in Eμ-*myc* mice deficient in *btk/tec* kinases.** (A) Eμ-*myc* Tg rescues B cell maturation in *btk*$^{-/-}$*tec*$^{-/-}$ mice. BM cells isolated from mice of the indicated genotypes (4–6 wk) were analyzed by flow cytometry for the expression of developmentally regulated surface markers. Cells falling in the live lymphocyte gate are shown. (B) Absence of Btk/Tec kinases accelerates tumor formation in Eμ-*myc* transgenic mice. Kaplan-Meier tumor-free estimates for mice of the indicated genotypes. Tumor-free survival in Eμ-*myc btk*$^{-/-}$/*tec*$^{+/-}$ and Eμ-*myc btk*$^{-/-}$/*tec*$^{-/-}$ mice was significantly reduced as compared with Eμ-*myc* mice.

sustained PLCγ activation, peak IP_3 production, and maximal release of $[Ca^{2+}]_i$ (see Fig. 8; for reviews see Rawlings, 1999; Hendriks and Middendorp, 2004).

To investigate whether Ca^{2+} signaling is affected during Myc-dependent differentiation, we labeled total BM cells from Eμ-*myc* Tg and Wt mice as well as Eμ-*myc*/RAG2$^{-/-}$ and RAG2$^{-/-}$ mice with the Ca^{2+}-binding dye indo-1 (June and Rabinovitch, 1990) and fluorescent-conjugated antibodies against B cell markers and measured the ability of B cell progenitors to flux Ca^{2+} after stimulation with the Ca^{2+} ionophore ionomycin or anti-IgM. Surprisingly, we find that B cell progenitors from both Eμ-*myc* Tg and Eμ-*myc*/RAG2$^{-/-}$ mice exhibit elevated basal $[Ca^{2+}]_i$ and prolonged duration of Ca^{2+} flux compared with Wt and RAG2$^{-/-}$ mice, respectively (Fig. 5 A and not depicted). Remarkably, Eμ-*myc* Tg also rescues peak and sustained $[Ca^{2+}]_i$ in B cells (before and after anti-μ stimulation) in the absence of Btk and Tec kinases (Eμ-*myc* Tg/*btk*$^{-/-}$/*tec*$^{-/-}$), which are the major mediators of sustained Ca^{2+} signaling downstream of the pre-BCR (Fig. 5 B). These results suggest that Myc amplifies $[Ca^{2+}]_i$ signaling in B cells downstream of the pre-BCR and Tec kinases.

We next determined whether the elevated Ca^{2+} flux we observe in Myc-expressing B cells results in changes in known nuclear mediators of Ca^{2+} signaling. In normal T and B cells,

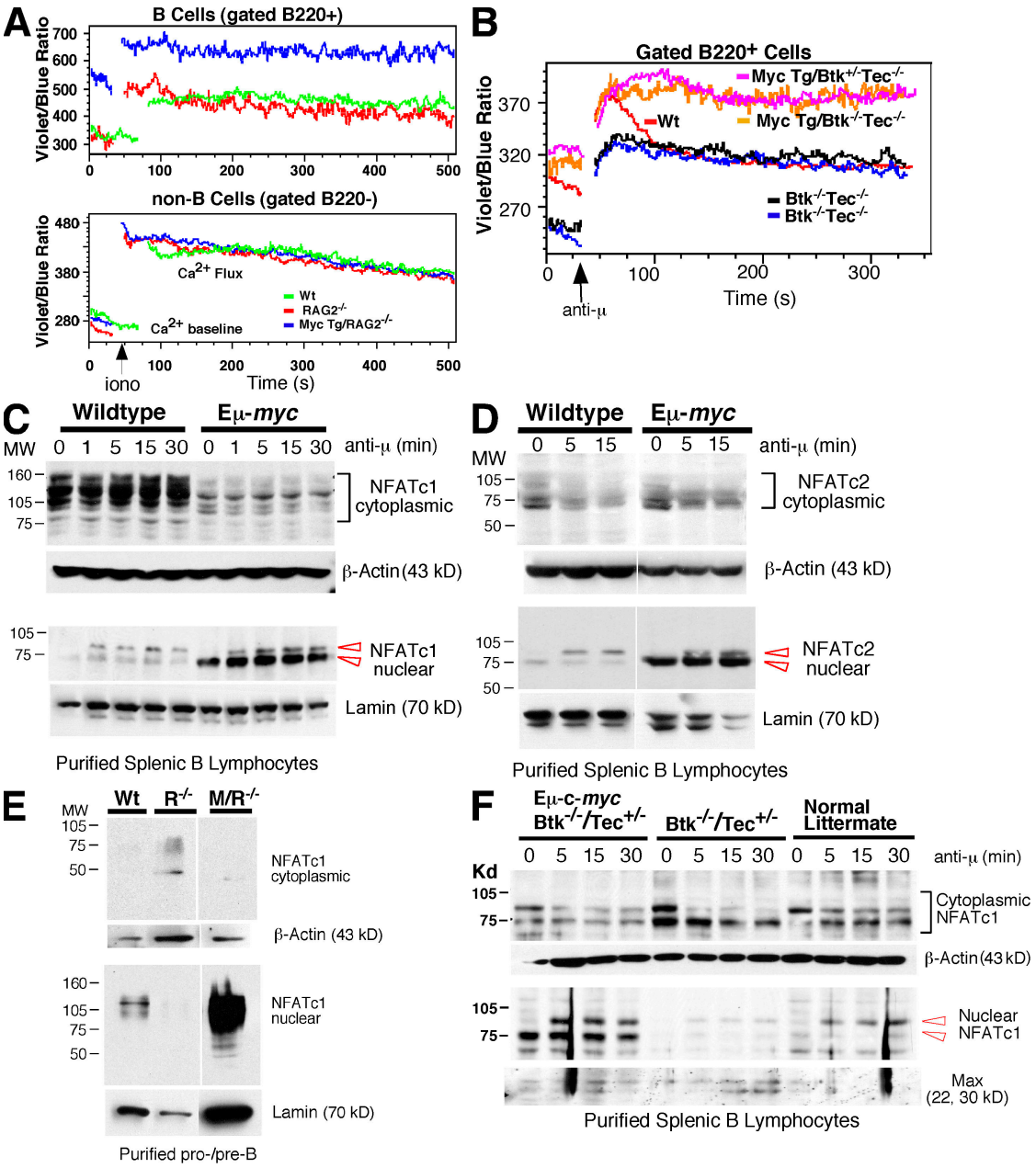

Figure 5. **Eμ-*myc* B cells exhibit elevated Ca^{2+} flux and enhanced NFATc nuclear translocation.** (A) BM cells from Wt, RAG2$^{-/-}$, or Eμ-*myc*/RAG2$^{-/-}$ mice were loaded with indo-1 dye and stained with αB220. Flow kinetics profiles are shown comparing the mean indo-1 ratio (violet/blue) of B220^{+} (top) and B220^{-} (bottom) cells as a function of time before and after stimulation with ionomycin. (B) Eμ-*myc* Tg rescues Ca^{2+} flux in Btk/Tec-null B cell progenitors. BM cells from mice of the indicated genotypes were loaded with indo-1 and stained with αB220 and αCD43. Kinetics profiles comparing the indo-1 fluorescence ratio of B220^{+} cells as a function of time before and after stimulation with anti-μ are shown. (C–F) B cells from Eμ-*myc*, Eμ-*myc*/RAG2$^{-/-}$, and Eμ-*myc*/*btk*$^{-/-}$*tec*$^{+/-}$ mice exhibit enhanced nuclear localization of NFATc. Cytoplasmic and nuclear extracts were prepared from splenic B cells stimulated with anti-μ for the indicated times (C, D, and F) or unstimulated purified B cell progenitors (E) and were size fractionated by SDS-PAGE. Western blot analysis was performed with αNFATc1 (C, E, and F) or αNFATc2 (D) or with loading controls β-actin (C–F), α-lamin (C–E), or α-Max (F). Adjacent panels depicted in D or E are from the same gel. White lines indicate that intervening lanes have been spliced out. R$^{-/-}$, RAG2$^{-/-}$; M/R$^{-/-}$, Eμ-*myc*/RAG2$^{-/-}$. NFAT isoforms are indicated by brackets or arrowheads.

Ca^{2+} influx activates the phosphatase calcineurin (Cn), which dephosphorylates the NFAT family of transcription factors (NFATc1–4), allowing them to translocate from the cytoplasm to the nucleus and activate transcription of target genes (for reviews see Crabtree, 2001; Im and Rao, 2004). We examined the translocation of NFAT in purified splenic B cells from Eμ-*myc* Tg and normal Wt littermates both before and after BCR cross-linking. Purified B cells from Wt littermates require 15 min of anti-IgM stimulation to achieve the maximal translocation of NFATc1 (Fig. 5 C and Fig. S5 C, available at http://www.jcb.org/cgi/content/full/jcb.200704173/DC1) and NFATc2 (Figs. 5 D and S5 D) to the nucleus. In contrast, B cells from Eμ-*myc* Tg mice have the majority of both NFATc1 and c2 in the nucleus, even before stimulation with anti-IgM. These effects are not the result of

increased NFAT expression in Eμ-*myc* B cells, as *NFATc* mRNA (Fig. S4 A) and protein levels (Fig. S5, A and B) are reduced or unchanged relative to Wt B cells. Myc expression also results in substantially increased nuclear NFATc1 translocation in unstimulated B cell progenitors from Eμ-*myc*/RAG2$^{-/-}$ compared with RAG2$^{-/-}$ mice (Figs. 5 E and S5 E) and rescues NFAT translocation in splenic B cells from Eμ-*myc*/*btk*$^{-/-}$*tec*$^{-/+}$ as compared with *btk*$^{-/-}$*tec*$^{-/+}$ mice (Figs. 5 F and S5 F). Transfection of Myc-null fibroblasts (HO.15 cells) with c-Myc (Shiio et al., 2002) results in greatly enhanced NFAT activity based on increased activation of an NFAT-luciferase reporter construct (Fig. S3 E), demonstrating that Myc also increases NFAT activity. These results suggest that the sustained increase in $[Ca^{2+}]_i$ signaling in Myc-expressing B cells has a major influence on key Ca^{2+}-regulated nuclear events.

To assess whether the elevated Ca^{2+} flux in Myc-expressing B cell progenitors may contribute to the abilities of Myc to stimulate maturation and proliferation, we first determined how $[Ca^{2+}]_i$ levels in these mice correlate with differentiation, proliferation, and survival status. We find that Ca^{2+} levels positively correlate with maturation and proliferation in Eμ-*myc*/RAG2$^{-/-}$ mice based on the down-regulation of CD43 on B220$^+$ cells and dilution of CFSE. B cell progenitors with the most mature phenotype (B220$^+$CD43$^-$) and highest proliferative capacity have the highest levels of Ca^{2+} flux, whereas the cells with the least mature phenotype (B220$^+$CD43$^{hi–mid}$) and lowest proliferative capacity have the lowest levels of Ca^{2+} flux (Fig. S3, A–C). The observed increase in $[Ca^{2+}]_i$ is not the result of differences in cell cycle status because gated G0/G1 cells from Eμ-*myc* Tg have consistently elevated $[Ca^{2+}]_i$ relative to G0/G1 cells from normal littermates (Fig. S3 D). These results suggest that there is a correlation between amplified Ca^{2+} signaling and the ability of Myc-expressing B cells to undergo differentiation and division.

We next examined whether normal Ca^{2+} signaling is required for maturation and division of Wt and Myc Tg pre–B cells. First, we determined whether impairing endogenous Myc expression results in impaired Ca^{2+} flux. Total BM cells from N-*myc*$^{fl/fl}$ c-*myc*$^{fl/fl}$ CD19cre$^-$ or CD19cre$^+$ mice were stimulated in vitro with anti-μ for 2 h to induce *myc* expression followed by ionomycin stimulation to induce Ca^{2+} flux. As shown in Fig. 6 A, both pre–B/immature B and mature B cell populations from N-*myc*$^{fl/fl}$ c-*myc*$^{fl/fl}$ CD19cre$^+$ mice exhibit reduced peak and sustained Ca^{2+} levels relative to CD19cre$^-$ mice. To determine whether a reduction of Ca^{2+} levels affects the ability of both Wt and Eμ-*myc* cells to proliferate and mature, we cultured total BM cells from Wt and Myc Tg mice in EGTA to limit the amount of available extracellular Ca^{2+} and assessed maturation and proliferative capacity after the addition of increasing doses of extracellular Ca^{2+}. As shown in Fig. S4 (B and C), chelation of Ca^{2+} with EGTA results in the impairment in Ca^{2+} flux and proliferative capacity after ionomycin stimulation. EGTA also blocks the ability of Wt B cell progenitors to mature from the B220$^+$CD43$^+$ stage to the B220$^+$CD43$^-$ stage (Fig. 6 B, first and second panels), which is rescued by the addition of extracellular Ca^{2+} (Fig. 6 B, third to fifth panels). B cell progenitors were unable to divide in low Ca^{2+} conditions based on limited CFSE dilution of live (TO-PRO-3) cells (Fig. 6 C, first and second panels), which is also rescued by the addition of extracellular Ca^{2+} (Fig. 6 C, third to fifth panels). Progenitors from Eμ-*myc*/RAG2$^{-/-}$ mice were also unable to mature (Fig. S4 D) or divide efficiently (not depicted) under low Ca^{2+} conditions.

As Eμ-*myc* B cells exhibit increased NFAT nuclear translocation, we also determined whether the Cn–NFAT pathway is required for the division of Wt and Eμ-*myc* B cells. Purified B cells from Wt and Eμ-*myc* mice were stimulated with anti-μ for 72 h in the presence or absence of cyclosporine A (CsA), a specific inhibitor of Cn. As shown in Fig. 6 D, Wt B cells undergo an average of four divisions (Fig. 6 D, left), and Eμ-*myc* B cells undergo an average of five divisions (Fig. 6 D, right) in response to anti-μ, whereas cell division is completely inhibited by CsA. Collectively, these results suggest that normal Ca^{2+} signaling is required for pre-BCR–mediated pre–B cell proliferation and maturation and for Myc to stimulate the differentiation of B cell progenitors.

Myc regulates Ca^{2+} efflux

The increase in $[Ca^{2+}]_i$ that occurs in response to stimuli such as BCR ligation is transient, in part because Ca^{2+} is resequestered into the endoplasmic reticulum by the sarcoplasmic ER Ca^{2+} ATPase (SERCA) or is extruded from the cell by plasma membrane Ca^{2+}-ATPase (PMCA) pumps. Because Myc amplifies $[Ca^{2+}]_i$ in B cells in the absence of Btk and Tec (which regulate influx), we hypothesized that Myc could be altering the extent of Ca^{2+} efflux. First, we measured the relative expression of *PMCA1*, *PMCA4*, and *SERCA3*, the respective pumps expressed in B lineage cells (Chen et al., 2004). Although we did not find consistent differences in the expression of *PMCA1* and *serca3* in mature B cells from Eμ-*myc* mice relative to Wt mice (unpublished data), levels of *PMCA4* mRNA are significantly decreased in Eμ-*myc* mature B and Eμ-*myc*/RAG2$^{-/-}$ pro–B cells (Fig. 7 A), whereas *PMCA4* mRNA is increased in sorted pro–B cells from N-*myc*$^{fl/fl}$ c-*myc*$^{fl/fl}$ CD19cre$^+$ versus CD19cre$^-$ mice (Fig. S4 E). The decrease in *PMCA4* expression correlates with a decrease in total PMCA protein (Fig. 7 B) and export of Ca^{2+} across the plasma membrane in purified B cells from Eμ-*myc* mice relative to Wt mice in response to anti-μ (Fig. 7 C), as measured by fluorometric analysis of extracellular media containing a membrane-impermeable version of the Ca^{2+}-binding Indo-1 dye. These results suggest that Myc negatively regulates Ca^{2+} extrusion in B cells and are consistent with a recent report that Myc interacts with the human *PMCA4b* promoter, resulting in decreased *PMCA4b* expression (Zeller et al., 2006). Indeed, we also find using chromatin immunoprecipitation (ChIP) that Myc interacts within the homologous region in the mouse PMCA4 promoter (Fig. S4 F).

To determine whether reduced *PMCA4b* expression in Myc-expressing cells is important for Myc-induced proliferation, we infected BM cells from Wt or Eμ-*myc* mice with murine stem cell virus (MSCV) retroviruses containing internal ribosomal entry site (IRES)–GFP and human *PMCA4b* cDNA (MSCV-*PMCA4b*-GFP) or vector alone (MSCV-GFP). Analysis of the Phoenix retroviral packaging cell line indicates that MSCV-*PMCA4b*-GFP$^+$ cells exhibit a substantially decreased baseline and peak $[Ca^{2+}]_i$ after ionomycin stimulation relative to GFP$^-$ cells,

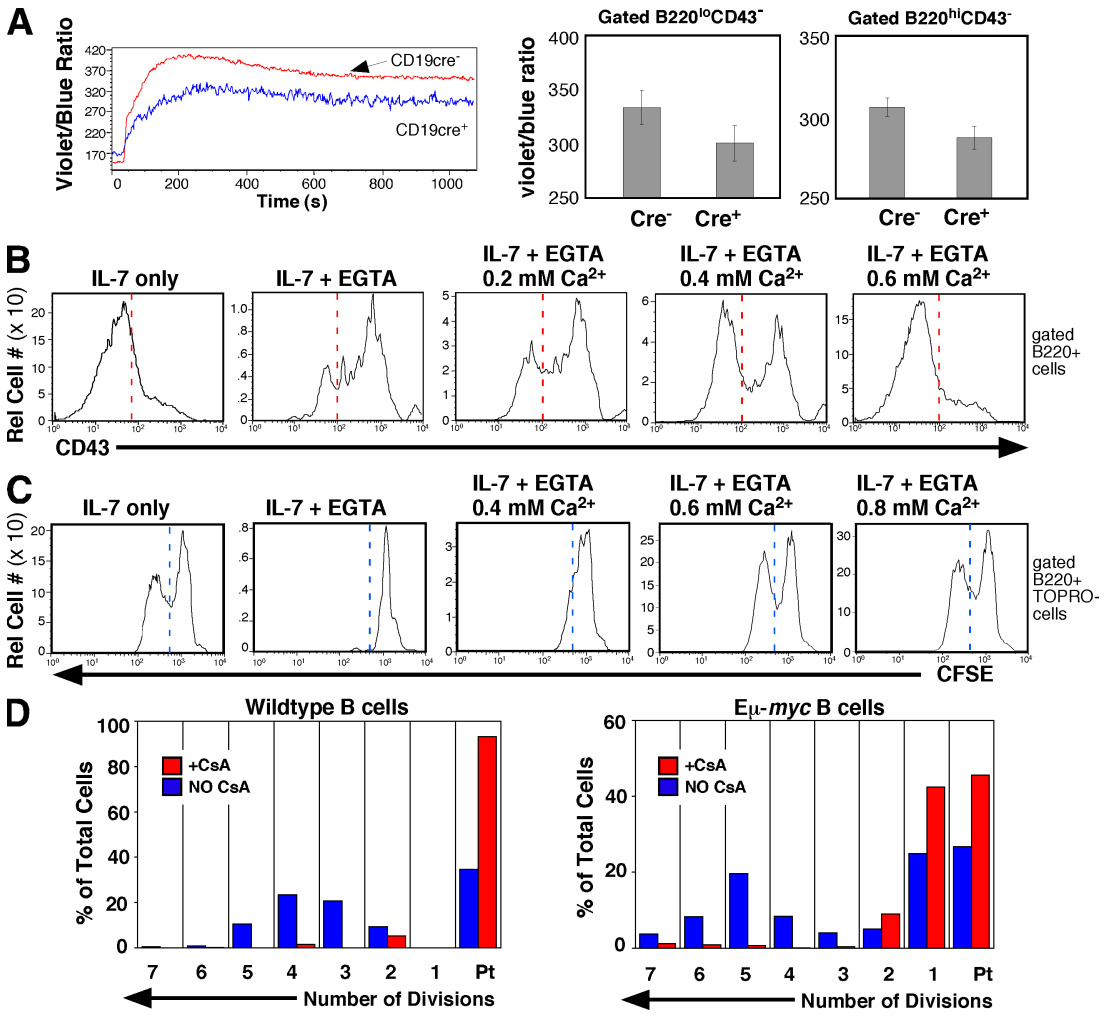

Figure 6. **Calcium signaling is required for pre–B cell development and for Myc-mediated maturation of RAG2-null pro–B cells.** (A) BM cells from the indicated mice were loaded with indo-1, stained with αB220 and αCD43, and preincubated with anti-μ for 2–3 h to up-regulate *myc*. (left) Representative kinetics profile comparing the mean indo-1 ratio versus time after stimulation of anti-μ–pretreated cells with ionomycin. (right) Bars represent the mean fluorescence ratio ± SEM (error bars) after ionomycin-stimulated Ca^{2+} flux of $B220^{lo}CD43^{-}$ BM cells (left; $n = 4$ mice/group) or $B220^{hi}CD43^{-}$ cells (right; $n = 6$ mice/group). (B) Wt BM cells were stained with CFSE and cultured for 48 h with IL-7 in the presence or absence of 1 mM EGTA and the indicated concentrations of $CaCl_2$. Representative histograms of CD43 expression on gated $B220^{+}$ cells are shown. (C) IL-7–induced proliferation of CFSE-stained cultures from B. CFSE dilution histograms of gated $B220^{+}$ TO-PRO-3^{-} cells are shown. Results are representative of three separate experiments. (B and C) The vertical dotted lines denote an equivalent location on the x axis of each panel for orientation. (D) The Cn–NFAT pathway is required for the proliferation of Wt and Eμ-*myc* B cells. Splenocytes from Wt (left) or Eμ-*myc* (right) mice were stained with CFSE and cultured with anti-μ in the presence or absence of CsA for 72 h. Panels represent the number of $B220^{+}$ cell divisions after MODFIT analysis. Results are representative of two separate experiments.

whereas MSCV-GFP^{+} cells flux normally (Fig. 7 D). Infection of Wt and Eμ-*myc* BM with MSCV-*PMCA4b*-GFP virus results in increased *hPMCA4b* expression over MSCV-GFP–infected cells by real-time PCR (Fig. 7 E). MSCV-GFP–infected Wt and Eμ-*myc* pre–B cells ($B220^{+}GFP^{+}$) divide normally in response to IL-7 in vitro based on considerable dilution of the CFSE-like SNARF-1 dye. In contrast, B cell proliferation is inhibited in MSCV-*PMCA4b*-GFP–infected Wt and Eμ-*myc* B cells in a dose-dependent manner (Fig. 7 F and not depicted).

Discussion

Myc stimulates B lymphocyte development

The roles of Myc proteins in cell differentiation remains one of the most controversial issues in Myc biology. Early studies performed in cell lines and more recent studies in primary keratinocytes resulted in the prevailing view that Myc stimulates cell cycle entry while inhibiting differentiation (for review see Pelengaris et al., 2002). However, in primary chicken and murine B cells engineered to overexpress *myc* and in humans with Burkitt's lymphoma, B lymphocytes mature to the Ig^{+} B cell stage relatively unperturbed despite the constitutive overexpression of *myc* throughout B cell development (Langdon et al., 1986; Thompson et al., 1987). These results suggest that B cells are able to mature relatively normally despite the presence of deregulated Myc.

In this study, we took a genetic approach to address the roles of Myc in the differentiation of mammalian cells using primary B cells. First, we found that conditional *myc* deletion significantly inhibits B cell development at the pro–B to pre–B cell transition (Fig. 1 B), which is the stage at which the combined

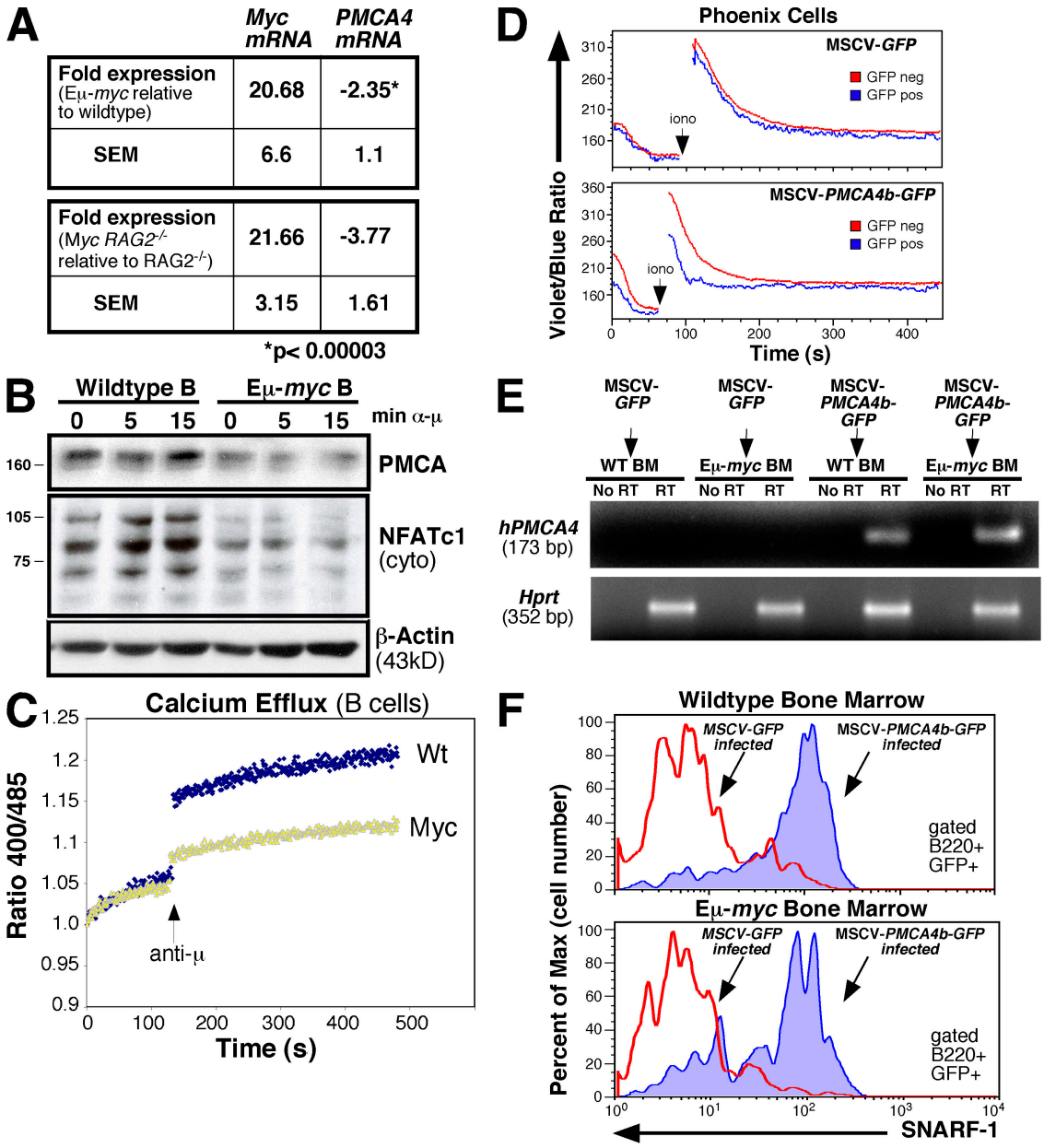

Figure 7. **Reduced PMCA expression in Eμ-*myc* B cells correlates with decreased Ca^{2+} efflux and increased proliferation.** (A) Real-time PCR analysis of c-*myc* and *PMCA4* message from purified splenic B cells (top) or pro–/pre–B-like cells (bottom). The fold expression ratio (Eμ-*myc*/Wt or Eμ-*myc*–RAG2$^{-/-}$/RAG2$^{-/-}$) of c-*myc* and *PMCA4* message is shown. Values represent the mean ± SEM obtained from three (top) or two experiments (bottom). (B) Reduced PMCA protein in unstimulated and anti-μ–treated Eμ-*myc* splenic B cells correlates with decreased cytoplasmic NFATc1 (increased NFATc1 nuclear translocation) as compared with Wt littermate controls. Cytoplasmic extracts were analyzed by immunoblotting. (C) Ca^{2+} efflux from splenic B cells purified from Eμ-*myc* and Wt mice measured before and after stimulation with anti-μ (arrow). A representative kinetics profile (Ca^{2+} extrusion rate) comparing the extracellular indo-1 fluorescence ratio as a function of time is shown. (D) The enforced expression of *PMCA4b* results in impaired Ca^{2+} flux. MSCV-*GFP* and MSCV-*PMCA4b-GFP*–transfected Phoenix cells were loaded with indo-1 after collecting viral supernatants for the infection of BM cultures depicted in F. Flow cytometric kinetics profiles of MSCV-*GFP* control (top) and MSCV-*PMCA4b-GFP* (bottom) cells comparing Ca^{2+} mobilization of GFP^- versus GFP^+ cells as a function of time before and after stimulation with ionomycin. (E) RT-PCR analysis confirming the specific expression of human *PMCA4* message from MSCV-*PMCA4b-GFP*–infected Wt and Eμ-*myc* BM depicted in F. *hprt* was amplified as a loading control. (F) The enforced expression of *PMCA4b* inhibits the proliferation of Wt and Eμ-*myc* BM B cells. BM cells infected with MSCV-*GFP* or MSCV-*PMCA4b-GFP* were labeled with SNARF-1 and cultured in the presence of IL-7 for 48 h. Cultures were stained with αB220 and analyzed by flow cytometry. Single-parameter SNARF-1 dilution histograms of gated $B220^+GFP^+$ cells are shown. Results are representative of two separate experiments.

signaling from the pre-BCR and IL-7 normally induce c- and N-*myc* expression. Second, to distinguish the ability of Myc to drive the proliferation of postdifferentiated cells from its ability to initiate a differentiation program, we asked whether Myc could rescue differentiation on two genetic backgrounds (RAG2$^{-/-}$ and *btk*$^{-/-}$/*tec*$^{-/-}$) whereby B cell development is blocked just before the stages at which c- and N-*myc* are normally expressed. We found that the Eμ-*myc* Tg efficiently stimulated the differentiation and expansion of pre–B-like cells from pro–B cells in the absence of pre-BCR formation (in RAG2$^{-/-}$ mice). Additionally,

we found that Myc can rescue B cell development to the IgM^+ immature B cell stage in the context of a *btk*$^{-/-}$/*tec*$^{-/-}$ background, whereby B cell development is nearly completely blocked at the large pre–B cell stage. These results collectively provide genetic evidence that Myc acts downstream of the pre-BCR and Btk/Tec to stimulate pre–B cell development and are consistent with previous studies suggesting that the pre-BCR is required for *myc* induction and pre–B cell development (Zimmerman and Alt, 1990; for review see Hendriks and Middendorp, 2004).

The notion that Myc may initiate differentiation was first proposed by Gandarillas and Watt (1997) in keratinocytes in vitro. Recent studies have suggested roles for Myc in inducing the differentiation of hematopoietic and epidermal stem cells, in part by regulating the expression of adhesion molecules, thus releasing them from a differentiation-inhibiting niche (Murphy et al., 2005). In this study, we show that constitutive Myc can act in a cell-autonomous manner to rescue differentiation in lineage-committed progenitor cells. These results collectively suggest that the phenotypic consequences of Myc during development may depend on the differentiation status of the cell: Myc expression in stem cells and lineage-committed progenitors results in differentiation, whereas Myc expression in mature postmitotic cells results in reentry into the cell cycle and inhibition of terminal differentiation.

Deregulated Myc synergizes with the loss of Tec kinase function during lymphoma formation

Although *btk*-null or *btk/tec* double-null mice do not spontaneously develop pre–B cell tumors, the absence of both *btk* and *SLP-65* significantly enhances the incidence of pre–B cell leukemia as compared with *SLP-65*–null mice (Hendriks and Kersseboom, 2005). Although the exact mechanism of tumor suppression by Tec family PTKs is not known, the loss of Btk and/or SLP-65 in B cells results in sustained IL-7 receptor (IL-7R) expression and an increased proliferative and/or survival response to IL-7. Here, we show that loss of Btk/Tec significantly accelerates B cell tumor formation in Eμ-*myc* mice (Fig. 4 B). In addition, we find that Eμ-*myc* Tg substantially increases the proliferative potential of B cell progenitors in response to IL-7, whereas decreasing *myc* expression inhibits IL-7–mediated proliferation. Thus, sustained IL-7R expression in *tec/btk*-null mice, in cooperation with constitutive Myc activity as occurs in Burkitt's lymphoma, substantially increases the pool of dividing cells that is capable of acquiring epigenetic alterations that promote tumorigenesis. We conclude that Tec PTKs act as tumor suppressors that attenuate deregulated c-*myc* and that IL-7 synergizes with Myc to increase the pool of dividing B cell progenitors. The ability of Myc to drive differentiation to the IgM-positive stage in Btk$^{-/-}$/Tec$^{-/-}$ mice while having accelerated transformation further suggests that it is not the inhibition of maturation itself but rather the degree of growth factor responsiveness that determines tumor susceptibility. Consistent with the latter notion, loss of Jak3 kinase, an essential IL-7 signaling molecule, reduces the transforming potential of the Eμ-*myc* Tg (Dillon and Schlissel, 2002).

Myc regulates Ca^{2+} signaling and NFAT translocation during B cell development

Because Ca^{2+} signaling is important for virtually all aspects of embryogenesis (for review see Webb and Miller, 2003) and pre-BCR and Btk stimulate Ca^{2+} signaling pathways, we were prompted to investigate how Ca^{2+} signals were affected during Myc-dependent B cell development. Surprisingly, we found that both basal $[Ca^{2+}]_i$ levels and the duration of Ca^{2+} flux are elevated in B cells from Eμ-*myc* Tg and Eμ-*myc*/RAG2$^{-/-}$ mice. Furthermore, an increase in the relative level of $[Ca^{2+}]_i$ in Eμ-*myc*/RAG2$^{-/-}$ Tg mice positively correlates with increased proliferation and differentiation and is required for Myc to stimulate B cell development and proliferation. The increase in $[Ca^{2+}]_i$ level may occur by down-regulation of the Ca^{2+} efflux pump PMCA4b because Myc interacts with the *PMCA4b* promoter, and both *PMCA4b* expression and Ca^{2+} efflux are decreased in Eμ-*myc* B cells. Moreover, enforced *PMCA4b* expression inhibits Myc-induced cell proliferation. These results are consistent with a study in developing T lymphocytes in the thymus, which depend on Ca^{2+} signaling during the maturation and expansion of $CD4^-CD8^-$ pre–T cells after rearrangement of the T cell receptor β chain and formation of the pre–T cell receptor (Aifantis et al., 2001). In addition, gene-targeted mutations in other genes involved in Ca^{2+} signaling, including the Src family PTKs Lyn/Fyn/Blk, Syk, SLP-65, LAT (linker for activation of T cells), Btk/Tec, the p85 subunit of PI3K (Fruman et al., 1999), and PLCγ1/2 (Wen et al., 2004), also result in impaired B cell development at the pre–B cell stage. Altogether, these results strongly support a role for Myc and Ca^{2+} signaling in the maturation of pre–B cells.

A study in primary B lymphocytes indicates that the amplitude and duration of Ca^{2+} signals have profound influences on the type of transcriptional response (Dolmetsch et al., 1997). For example, NF-κB and JNK are selectively activated by a large transient $[Ca^{2+}]_i$ rise, whereas NFAT is activated by lower but sustained $[Ca^{2+}]_i$ levels. We also find that B cells from Eμ-*myc* Tg mice, which exhibit elevated, sustained $[Ca^{2+}]_i$ levels, also exhibit increased NFAT translocation even in the absence of upstream signals from the pre-BCR and BCR. In addition, B cell nuclear fractions from Myc Tg mice appear to contain mostly the short isoform of NFATc1 (NFATc1A; Fig. 5), which, in contrast to the other NFATc1 isoforms (NFATc1B and c1C), does not promote apoptosis in lymphocytes (Chuvpilo et al., 2002). These results suggest that the elevated $[Ca^{2+}]_i$ in Myc-expressing B cells has profound influences on transcriptional and biological responses as well. Indeed, we find that anti-IgM–induced B cell proliferation of both Wt and Myc Tg B cells is completely abrogated by treatment of cells with CsA, and a recent study indicates that the B cell–specific deletion of Cn results in defects in B cell proliferation and function (Winslow et al., 2006).

Implications of Myc-regulated Ca^{2+} signaling

One common feature of many types of cancers is their reduced dependence on external growth factors, and Myc-induced tumors share this property. Indeed, Myc activates at least three genetic programs that are normally growth factor dependent, including cyclin E/Cdk2 kinase, E2F-dependent transcription, and protein

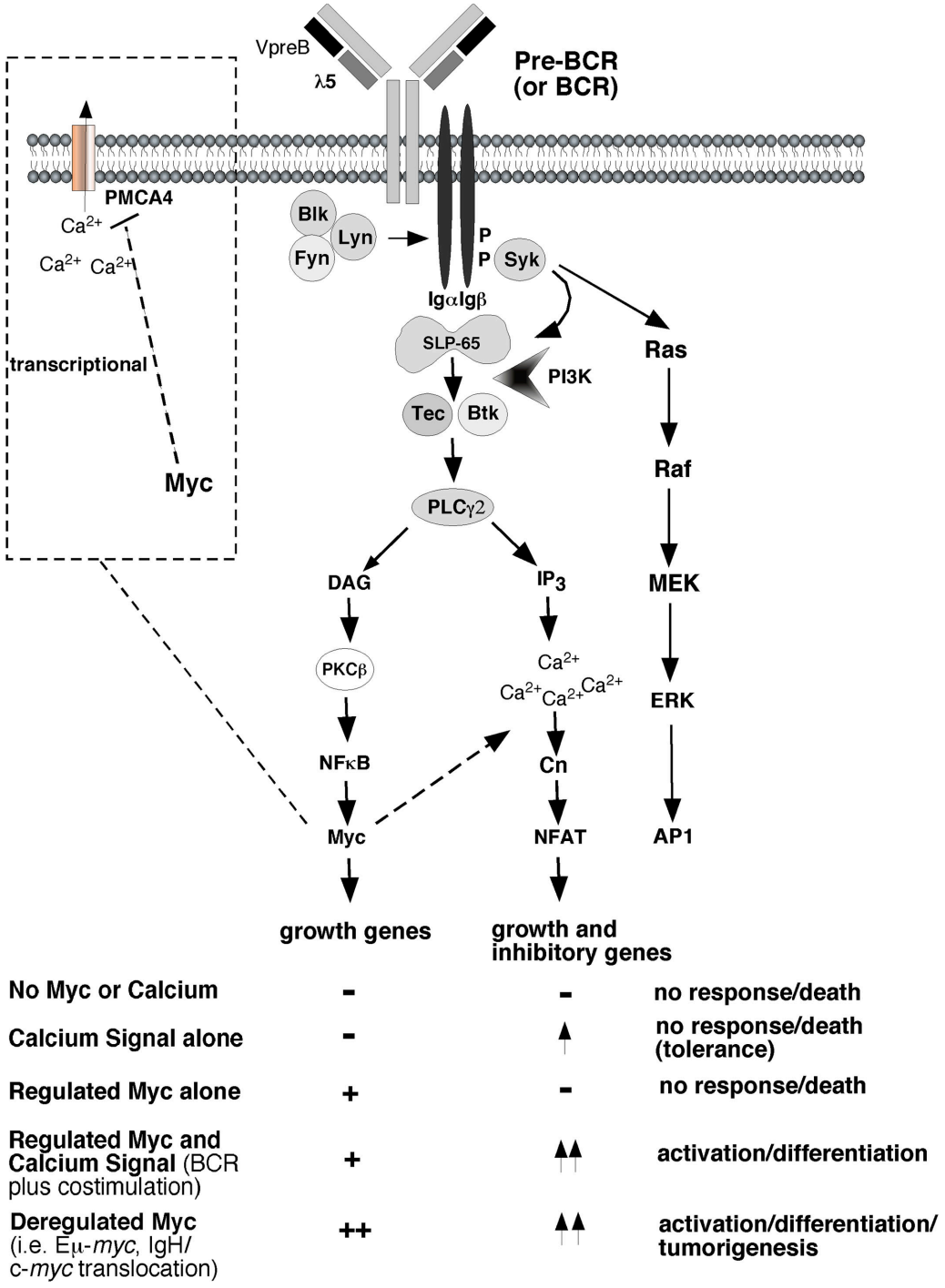

Figure 8. **Model of Myc and Ca^{2+} signaling events downstream of the pre-BCR/BCR.** Engagement of the pre-BCR/BCR results in the recruitment of Src family kinases (Blk, Lyn, and Fyn), phosphorylation of the Igα–Igβ complex, and formation of a Ca^{2+} signaling module containing SLP-65, PI3K, Btk/Tec, and PLCγ. Full activation of PLCγ by Btk results in IP_3-mediated Ca^{2+} release from the ER, resulting in activation of the Cn–NFAT signaling pathway. PKCβ activation by Ca^{2+} and DAG leads to the nuclear translocation of NF-κB and the induction of *myc* expression. Our results implicate Myc in amplifying $[Ca^{2+}]_i$ by decreasing PMCA4-mediated Ca^{2+} efflux, thereby promoting optimal NFAT-dependent proliferation, differentiation, and immunogenic B cell responses. Induction of low level Ca^{2+} signals or Myc signaling alone results in a tolerogenic and/or apoptotic response, whereas Myc activation together with sustained Ca^{2+}/NFAT signals or constitutive Myc signaling alone promotes B cell activation/differentiation or tumorigenesis.

synthesis pathways (for review see Eisenman, 2001). How can one transcription factor with limited target gene specificity induce so many biochemical and biological changes that are normally dependent on multiple signaling pathways? Our results suggest that although Myc directly stimulates the expression of many E box–containing genes, Myc also increases sustained $[Ca^{2+}]_i$ and enhances NFAT translocation (Fig. 8). This allows for the concurrent activation of Ca^{2+}-dependent target genes even in the apparent absence of upstream mediators of Ca^{2+} signaling, as might occur under conditions of poor growth factor availability

or limited extracellular Ca^{2+}. The synergy between Myc and $[Ca^{2+}]_i$ to stimulate B cell development and proliferation are strikingly similar to the signaling requirements underlying immunogenic versus tolerogenic responses to antigen in B lymphocytes. Although activation of Myc alone or a low level Ca^{2+} signal alone provokes apoptosis or anergy (tolerance; Glynne et al., 2000), Myc expression in conjunction with a sustained Ca^{2+}/NFAT signal results in a mitogenic response and immunity. Here, we find that Myc amplifies $[Ca^{2+}]_i$, thus tuning levels into the range required for optimal NFAT activation and translocation. The unique function of Myc to amplify Ca^{2+} signaling may help explain why transformed cells are relatively resistant to low growth factor and Ca^{2+} conditions (Whitfield, 1992) despite known requirements for Ca^{2+} signaling during G1→S transition.

Materials and methods

Mice

C57BL/6 Eμ-*myc* transgenic mice were obtained from Jackson ImmunoResearch Laboratories and were genotyped by PCR according to instructions from the supplier. To generate mice carrying conditionally inactivated c- and N-*myc* genes, mice carrying a floxed c-*myc* allele (c-$myc^{fl/fl}$; de Alboran et al., 2001) were bred to N-$myc^{fl/fl}$ mice (Knoepfler et al., 2002) expressing the *cre* recombinase Tg under the control of the CD19 promoter (Rickert et al., 1997). *btk/tec*-deficient mice have been described previously (Ellmeier et al., 2000). Mice were housed under specific pathogen-free conditions. All mouse procedures were approved by the University of Washington Institutional Animal Care and Use Committee.

Cell culture

For cell division experiments, cells were stained with CFSE according to the manufacturers' instructions (Invitrogen). CFSE-labeled cells were cultured in complete RPMI + 10% FBS (Hyclone) in the presence or absence of 10 ng/ml murine recombinant IL-7 (R&D Systems) or 5 μg/ml anti-μ (F(ab')2 fragment; Thermo Fisher Scientific) for the indicated times at 37°C and 5% CO_2. In some experiments, EGTA was added at a final concentration of 0.5, 0.75, or 1 mM to IL-7–driven cultures in the presence or absence of 0.2, 0.4, or 0.6 mM $CaCl_2$, and cyclosporine was added at a final concentration of 100 ng/ml to anti-μ–driven cultures. Thereafter, the cells were stained with the indicated antibodies for analysis by FACS or harvested for measurement of $[Ca^{2+}]_i$ (see section Measurement of intracellular calcium and DNA content). The vital dye TO-PRO-3 (Invitrogen) was added to the indicated samples (1-nM final concentration) before acquisition to distinguish live and apoptotic cells. The number of discrete CFSE peaks was determined using MODFIT software (Verity Software House).

The Myc-null and Myc-expressing fibroblast cell lines HO.15 and HO.15 + c-Myc, respectively, and the Phoenix packaging cell line were grown in DME supplemented with 10% FCS, glutamine, penicillin, streptomycin, and essential amino acids. For retroviral gene transfer into primary BM cells, human *PMCA4b* cDNA was subcloned into the HpaI site of the modified MSCV MIG vector upstream of the EGFP gene and IRES. The MSCV vector carrying only the IRES-EGFP cassette was used as a control. The cDNA of human *PMCA4b* was provided by M. Husain (Department of Physiology, University of Toronto, Toronto, Canada; Heim et al., 1992). Ecotropic viral stocks were generated by Ca^{2+} phosphate–mediated transfection of subconfluent Phoenix cells in the presence of chloroquine. Viral supernatant was collected and filtered after 3 d. For infection of Wt or Myc Tg BM, ∼15×10^6 cells were plated per well of a six-well plate and infected 48 h later with 4 ml of fresh viral supernatant and 4 μg/ml polybrene by spinoculation. Two rounds of infection were performed, and cells were then labeled with 1 μM SNARF-1 (S-22801; Invitrogen) for 15 min at room temperature. Cells were washed twice with complete RPMI + 10% FCS and cultured in fresh medium containing 10 ng/ml IL-7 for an additional 48 h. Thereafter, the cells were stained with αB220-phycoerythrin (PE) for analysis of $B220^+$ GFP^+ cell division by FACS.

Flow cytometric analysis

Single-cell suspensions were prepared and analyzed by flow cytometry as previously described (Iritani et al., 1997). The majority of antibodies used in this study are referenced in Iritani et al. (1997). Additional antibody conjugates used in this study include B220-PE-Cy-5.5 (eBioscience), FITC anti–mouse CD21, biotin anti–mouse CD22.2, biotin anti–mouse IA^b (BD Biosciences), FITC–annexin V (Invitrogen), IgM-PE-Cy7 (SouthernBiotech), and IgD-FITC (BD Biosciences). Cytometry was performed on FACScan and LSR flow cytometers (BD Biosciences). Data were analyzed using CellQuest (Becton Dickinson) and FlowJo (version 6.3.2; Tree Star, Inc.) softwares. To determine relative numbers of B lineage cells in each population (Fig. 1 B), percentages from flow cytometry were multiplied by the total BM cellularity to obtain absolute numbers of pro–B cells ($B220^+CD43^+$), pre–B cells ($B220^+CD43^-$), immature B cells ($B220^{lo}IgM^+$), and mature B cells ($B220^{hi}IgM^+$). To determine relative numbers of peripheral B2 B cells in each population (Fig. 2 A), percentages from flow cytometry were multiplied by the total spleen cellularity to obtain absolute numbers of total B cells ($B220^+IgM^+$), follicular mature ($IgM^{lo}IgD^{hi}$), T2 ($IgM^{hi}IgD^{hi}$), and T1/MZ ($IgM^{hi}IgD^{lo}$) B cells.

Measurement of intracellular Ca^{2+} and DNA content

For measurement of $[Ca^{2+}]_i$, cells were washed and resuspended in 0.5 ml HBSS containing 3% FBS at 10^6–10^7 cells/ml (for harvested BM cultures) or 5×10^7–8×10^7 cells/ml (for freshly isolated BM). EGTA-treated cell cultures were resuspended in Ca^{2+}-free HBSS/3% FBS. Indo-1–acetoxymethyl (pentaacetoxymethyl ester; Sigma-Aldrich) was added at a final concentration of 10–20 μM, and incubation was performed for 30 min at 37°C. The indo-1 fluorescence ratio (400:530 nm) of the cells was acquired as a function of time using a flow cytometer (BD-LSR I; Becton Dickinson). For each experiment, collection of a 30-s baseline measurement was followed by stimulation with either 25 μg/ml anti-μ or 1 μg/ml ionomycin (EMD) as indicated. For pre-BCR cross-linking of c- and N-*myc*–deficient or Wt BM, indo-1–loaded cells were first preincubated with 25 μg/ml anti-μ for 2–3 h at 37°C.

For simultaneous analyses of Ca^{2+} flux and DNA content, fluo-4 Ca^{2+}-binding dye (Invitrogen) was added at a final concentration of 1 μM in place of indo-1–acetoxymethyl. The cells were washed twice with HBSS/3% FBS and stained with the indicated antibody conjugates at room temperature for 45 min followed by Hoescht (Invitrogen) for 45 min at 37°C. Thereafter, the cells were washed twice, resuspended in a 1–2-ml final volume, and maintained at 37°C for 5 min before and during analysis of $[Ca^{2+}]_i$.

Measurement of extracellular Ca^{2+} $[Ca^{2+}]_o$

Ca^{2+} efflux was measured with a cell-impermeable form of indo-1 (5-μM final concentration; Invitrogen). 10^7 purified splenic B cells were washed twice with Na^+-free/Ca^{2+}-free efflux buffer (modified from Chen et al., 2004) and resuspended in 2 ml efflux buffer (10 mM Hepes, pH 7.4, 1 mM $MgCl_2$, 5 mM KCl, 135 mM choline chloride, 10 mM glucose, and 0.1% BSA). Fluorescence of cell suspensions was detected with a Fluorescence Master Series fluorometer (Photon Technology International) at an excitation wavelength of 350 nm and emission wavelengths of 400 and 485 nm. Collection of a baseline measurement was followed by stimulation with 10 μg/ml anti-μ (F(ab')2 fragment), and ratiometric Ca^{2+} values (400:485 nm) were plotted as a function of time.

Reporter gene assays

For NFAT-luciferase assays, HO.15 (Myc null) or HO.15 + c-Myc fibroblasts were plated in 24-well tissue culture dishes at 90% confluence and, 24 h later, were transfected in triplicate with pNFAT-luciferase plasmid or pCIS-CK negative control plasmid containing the luciferase reporter gene without any cis-acting elements (Stratagene) and the pRL Renilla luciferase control reporter vector (Promega) using LipofectAMINE (Invitrogen) according to the manufacturer's instructions. Treatment with 60 ng/ml PMA + 1 μg/ml ionomycin or PMA/ionomycin + 100 ng/ml CsA was performed 18 h after transfection. After 6 h, luciferase assays were performed with a luminometer (Monolight 1500; Analytical Luminescence Laboratories) and the Dual Luciferase Reporter assay system (Promega). Firefly luciferase values for each transfection were normalized to Renilla luciferase activity (pRL), and data were expressed as relative luciferase activity versus that obtained with the pCIS-CK negative control plasmid. Mean values of a representative experiment of three performed are displayed ± SEM.

In vivo BrdU labeling

Mice were given water containing 0.8 mg/ml BrdU (Sigma-Aldrich) for 2 d. BM was harvested, surface stained for B220, and fixed, permeabilized, and treated with 30 μg DNase I (Sigma-Aldrich). Incorporation of BrdU into DNA was measured by flow cytometry using anti–BrdU-FITC (BD Biosciences) according to the manufacturer's protocol.

B cell purification

Single-cell suspensions of total splenocytes and BM cells were isolated as previously described (Iritani et al., 1997). B lymphocytes were enriched by

negative selection on magnetic microbeads coupled to rat anti–mouse CD43 (Miltenyi Biotec) or using the mouse B cell Negative Isolation kit (Invitrogen) according to protocols provided by the manufacturers. The recovered splenic B cells were rested in RPMI 1640 medium before stimulation for biochemical analyses or were washed into efflux buffer for Ca^{2+} efflux assays. B lineage cells were enriched from total BM by positive selection on magnetic beads coupled to CD45R/B220 (Invitrogen) or CD19 (Miltenyi Biotec) according to the manufacturers' instructions or by cell sorting on a FACSaria (BD Biosciences).

Western blot analysis

Purified splenic B cells were stimulated with 25 μg/ml anti-μ (F(ab') 2 fragment) in serum-free RPMI medium. At the indicated time points, the cells were washed twice in ice-cold PBS and resuspended in hypotonic buffer containing protease inhibitors. Cytoplasmic and nuclear extracts were prepared by the method of Dolmetsch et al. (1997). SDS-PAGE and Western blotting were performed using standard techniques. Anti-NFATc1, anti-NFATc2, anti–β-actin, anti-Max, and donkey anti–goat IgG-HRP were purchased from Santa Cruz Biotechnology, Inc. Rabbit anti–mouse IgG HRP secondary antibody was purchased from Invitrogen. Goat anti–rabbit IgG HRP secondary antibody was purchased from Bio-Rad Laboratories. Anti-PMCA monoclonal antibody (clone 5F10) was purchased from Millipore. Anti–lamin A/C antibody was purchased from Cell Signaling Technology. Anti–α-tubulin monoclonal antibody was purchased from Sigma-Aldrich.

ChIP

Purified splenic B cells from Myc Tg mice were cross-linked with 1% formaldehyde for 10 min at 37°C. ChIP was performed with the ChIP assay kit (Millipore) according to the manufacturer's instructions using anti–c-Myc (N-262; Santa Cruz Biotechnology, Inc.) or control rabbit IgG (rIgG; Santa Cruz Biotechnology, Inc.) antibodies. After reversal of cross-links, DNA was precipitated and detected by qPCR with pairs of primers (underlined) specific to the mouse PMCA4b promoter (189-bp region beginning at –2,872 relative to the putative transcription start site and –4,285 relative to the translation start site: 5′-TAGGAGCAAGCTCAGCAGTTAGCAAGCGCTCACGTTCTAGAAACTTGTGTGTCCCTCAGTGCAGCAGGACTTTAGTGGATTCCTGAAACTGGAGGTCTCCATCACACGCTGTTACTTGAACAGGTATATGTCTCTGATTCTCCCGGAGCAGTTCTGTAGCGCTCTACCTTCTAATCTTCTGTGCCGGCT-3′) and the APEX1 promoter as a positive E-box control (*APEX* forward, 5′-TACCACGAACAACCCAGAACC-3′; *APEX* reverse, 5′-GTACCTGACCTCCCAACGAAG-3′). Real-time qPCR was used to quantify the fold enrichment relative to background detected with rabbit IgG for each primer set. The irrelevant gene 45S was amplified to normalize samples (*45S* forward, 5′-TGAATTGTGGCCCTGAGTGATAGG-3′; *45S* reverse, 5′-GAGTGGTGTTTGTGTGTGTTGG-3′).

Genomic PCR and RT-PCR

For PCR analysis of c-and N-*myc* alleles, single-cell suspensions of total BM from control or mutant mice were stained with anti-B220 and anti-CD43 antibodies, and cell sorting was performed on a FACSaria; alternatively, cells were magnetically labeled with CD19 microbeads and positively selected with an autoMACS Separator (Miltenyi Biotec). The FACS-sorted $B220^+CD43^-$ and $B220^+CD43^+$ populations were directly lysed in PCR lysis buffer (Iritani et al., 1999). Purified $CD19^+$ B lineage cells were cultured with 10 ng/ml IL-7 for 0, 15, or 22 h before lysis with PCR lysis buffer. The resulting DNA was used directly for PCR at 10,000 genomes/μl. Primers used to amplify the floxed undeleted and deleted c-and N-*myc* alleles have been described previously (de Alboran et al., 2001; Knoepfler et al., 2002). Deletion of *c-myc* was quantified by real-time PCR measurements of the c-$myc^{fl/fl}$ PCR product in the presence or absence of CD19cre. PCR analysis for D-J and V-D-J rearrangement of the Ig HC was performed as previously described (Iritani et al., 1999).

Real-time quantitative RT-PCR

RNA from purified Wt and Eμ-c-*myc* splenic B cells, Wt and Eμ-c-*myc* total BM, or FACS-sorted $B220^+$ Eμ-c-*myc*/$RAG2^{-/-}$, $RAG2^{-/-}$, and CD-19*cre* c-$myc^{fl/fl}$ N-$myc^{fl/fl}$ B cell progenitors was extracted using the RNAqueous-4PCR kit (Ambion). cDNA was generated using Superscript II Reverse Transcriptase (Invitrogen). Samples were normalized using *β-actin* (*β-actin* forward [5′-TCCTTCGTTGCCGGTCCAC-3′] and *β-actin* reverse [5′-ACCAGCGCAGCGATATCGTC-3′]) or *eif1α* (*eif1α* forward [5′-AGTGAGCACTGTTAAGAGACTGCC-3′] and *eif1α* reverse [5′-CGCAGCCAGATGACTAGAGTACAA-3′]). c-*myc* levels were determined using the following primers: c-*myc* forward (5′-ACCAACAGGAACTATGACCTC-3′) and c-*myc* reverse (5′-AAGGCAGTAGCGACCGCAAC-3′). The following primers were used for murine PMCA4: *mPMCA4* forward (5′-TCGTGACAGCCTTCAATGACTGGA-3′), *mPMCA4* reverse (5′-AGGTCACCGTATTTGATCTGGGCA-3′), and human PMCA4 (*hPMCA4* forward [5′-ATGACCCACCCTGAATTCGCCATA-3′] and *hPMCA4* reverse [5′-TGGTTGCAATCCACCGCATTGT-3′]).

Primers specific for the various isoforms of murine NFATc1 and NFATc2 have been described previously (Asagiri et al., 2005): *NFATc1A* forward (5′-GGTAACTCTGTCTTTCTAACCTTAAGCTC-3′), *NFATc1A* reverse (5′-GTGATGACCCCAGCATGCACCAGTCACAG-3′), *NFATc1B* forward (5′-CCCATCCGCCAGGCTACAGCCGCAGTAA-3′), *NFATc1B* reverse (5′-TTCGGTAAGTTGGGATTTCTGAGTGGTACC-3′), *NFATc1C* forward (5′-CCCATCCGCCAGGCTACAGCCGCAGTAA-3′), *NFATc1C* reverse (5′-TGAGTGGTACCAGATGTGGGTCCAGTTTAT-3′), *NFATc2* forward (5′-CACGCCTTCTACCAAGTACACAGGAT-3′), and *NFATc2* reverse (5′-ACAGTCGATGGTGGCTCTCATGTT-3′). Primers used to amplify hypoxanthine-guanine phosphoribosyl transferase (*hprt*) were as follows: *hprt* forward (5′-GTTGGATACAGGCCAGACTTTGTTG-3′) and *hprt* reverse (5′-GAGGGTAGGCTGGCCTATAGGCT-3′).

Primers used to amplify GL Igκ transcripts have been described previously (Hayashi et al., 2003). Quantitative deletion analysis of floxed c-*myc* alleles was performed using genomic DNA from FACS-sorted CD-$19cre^-$ or cre^+ c-$myc^{fl/fl}$ N-$myc^{fl/fl}$ pro– and pre–B cells and primers specific for the floxed c-*myc* allele (de Alboran et al., 2001) using 45S measurements to normalize. Experiments were performed using a real-time PCR system sequence detector (model 7300; Applied Biosystems) and a PCR system (Mx4000; Stratagene).

KLH immunization

Mice were immunized with KLH protein (Calbiochem) emulsified in complete Freund's adjuvant (CFA; 1:1 vol/vol mixture of 1 mg/ml of sterile protein solution–CFA) by subcutaneous injection at the base of the tail. Two injection sites were administered with 50 μl of the mixture. Mice were killed after 7 d. KLH-specific antibody production was measured with a KLH-coated ELISA system. For IgM, IgG1, and IgG2a measurements, serums were diluted 1:200, 1:135, and 1:135, respectively.

Statistical analysis

One-tailed *t* test was used for all analyses except the Kaplan-Meier analyses, in which we used Prism software (version 4; Graph Pad) to generate two-tailed p-values.

Image acquisition and manipulation

Developed films were scanned using Photoshop (version 8.0; Adobe), and adjustments of contrast and brightness were performed with Photoshop software. Scanned images were imported into Canvas (version 9.0.2; ACD Systems of America) for figure preparation. In reference to Fig. 5, the nuclear α-lamin control Western blots shown in Fig. 5 (C and E) and the β-actin control Western blot shown in Fig. 5 F were obtained by probing a separate gel. For evaluation of c- and N-*myc* deletion by densitometry (Fig. S1), band intensities representing the ratio of deleted to floxed alleles (with background subtracted) are shown below each lane and were quantified by densitometry on an imaging system (AlphaImager 3400; Alpha Innotech).

Online supplemental material

Fig. S1 shows the specific deletion of c- and N-*myc* in B lineage cells. Fig. S2 shows that the Eμ-*myc* Tg stimulates proliferation but not apoptosis of $RAG2^{-/-}$ B cell progenitors or Ig HC exclusion in Wt B cell progenitors. Fig. S3 shows that the elevated Ca^{2+} flux of Eμ-*myc* B cell progenitors correlates with increased maturation and proliferation and increased NFAT activity. Fig. S4 shows that chelation of Ca^{2+} impairs Ca^{2+} flux, maturation, and proliferation of Wt and Eμ-*myc* B cell progenitors in vitro, that Myc interacts with the mouse *PMCA4* promoter in Eμ-*myc* B cells, and real-time PCR analyses of *NFATc* message from purified splenic B cells and *PMCA4* message from c- and N-*myc*–deleted pro–B cells. Fig. S5 shows total levels of NFAT protein in whole cell lysates from Wt and Eμ-*myc* B cells and fractionation controls for the separation of cytoplasmic and nuclear fractions depicted in Fig. 5 (C–F). Online supplemental material is available at http://www.jcb.org/cgi/content/full/jcb.200704173/DC1.

We thank Alyson Fryer for her technical assistance and Dr. Mansoor Husain for the *hPMCA4* cDNA.

This study was supported by National Institutes of Health grant RO1AI0535468 and Royalty Research Fund 2773 to B.M. Iritani and National Cancer Institute grant R01CA20525 to R.N. Eisenman. R.N. Eisenman is an American Cancer Society Research Professor.

Submitted: 30 April 2007
Accepted: 22 October 2007

References

Aifantis, I., F. Gounari, L. Scorrano, C. Borowski, and H. von Boehmer. 2001. Constitutive pre-TCR signaling promotes differentiation through Ca2+ mobilization and activation of NF-kappaB and NFAT. *Nat. Immunol.* 2:403–409.

Asagiri M., K. Sato, T. Usami, S. Ochi, H. Nishina, H. Yoshida, I. Morita, E.F. Wagner, Mak, T.W., E. Serfling, and H. Takayanagi. 2005. Autoamplification of NFATc1 expression determines its essential role in bone homeostasis. *J. Exp. Med.* 202:1261–1269.

Charron, J., B.A. Malynn, P. Fisher, V. Stewart, L. Jeannotte, S.P. Goff, E.J. Robertson, and F.W. Alt. 1992. Embryonic lethality in mice homozygous for a targeted disruption of the N-myc gene. *Genes Dev.* 6:2248–2257.

Chen, J., P.A. McLean, B.G. Neel, G. Okunade, G.E. Shull, and H.H. Wortis. 2004. CD22 attenuates calcium signaling by potentiating plasma membrane calcium-ATPase activity. *Nat. Immunol.* 5:651–657.

Chuvpilo, S., E. Jankevics, D. Tyrsin, A. Akimzhanov, D. Moroz, M.K. Jha, J. Schulze-Luehrmann, B. Santner-Nanan, E. Feoktistova, T. Konig, et al. 2002. Autoregulation of NFATc1/A expression facilitates effector T cells to escape from rapid apoptosis. *Immunity*. 16:881–895.

Crabtree, G.R. 2001. Calcium, calcineurin, and the control of transcription. *J. Biol. Chem.* 276:2313–2316.

Davis, A.C., M. Wims, G.D. Spotts, S.R. Hann, and A. Bradley. 1993. A null c-myc mutation causes lethality before 10.5 days of gestation in homozygotes and reduced fertility in heterozygous female mice. *Genes Dev.* 7:671–682.

de Alboran, I.M., R.C. O'Hagan, F. Gartner, B. Malynn, L. Davidson, R. Rickert, K. Rajewsky, R.A. DePinho, and F.W. Alt. 2001. Analysis of C-MYC function in normal cells via conditional gene-targeted mutation. *Immunity*. 14:45–55.

Dillon, S.R., and M.S. Schlissel. 2002. Partial restoration of B cell development in Jak-3(−/−) mice achieved by co-expression of IgH and Eμ-*myc* transgenes. *Int. Immunol.* 14:893–904.

Dolmetsch, R.E., R.S. Lewis, C.C. Goodnow, and J.I. Healy. 1997. Differential activation of transcription factors induced by Ca2+ response amplitude and duration. *Nature*. 386:855–858.

Eisenman, R.N. 2001. Deconstructing myc. *Genes Dev.* 15:2023–2030.

Ellmeier, W., S. Jung, M.J. Sunshine, F. Hatam, Y. Xu, D. Baltimore, H. Mano, and D.R. Littman. 2000. Severe B cell deficiency in mice lacking the tec kinase family members Tec and Btk. *J. Exp. Med.* 192:1611–1624.

Fleming, H.E., and C.J. Paige. 2002. Cooperation between IL-7 and the pre-B cell receptor: a key to B cell selection. *Semin. Immunol.* 14:423–430.

Fluckiger, A.C., Z. Li, R.M. Kato, M.I. Wahl, H.D. Ochs, R. Longnecker, J.P. Kinet, O.N. Witte, A.M. Scharenberg, and D.J. Rawlings. 1998. Btk/Tec kinases regulate sustained increases in intracellular Ca2+ following B-cell receptor activation. *EMBO J.* 17:1973–1985.

Fruman, D.A., S.B. Snapper, C.M. Yballe, F.W. Alt, and L.C. Cantley. 1999. Phosphoinositide 3-kinase knockout mice: role of p85alpha in B cell development and proliferation. *Biochem. Soc. Trans.* 27:624–629.

Gandarillas, A., and F.M. Watt. 1997. c-Myc promotes differentiation of human epidermal stem cells. *Genes Dev.* 11:2869–2882.

Glynne, R., S. Akkaraju, J.I. Healy, J. Rayner, C.C. Goodnow, and D.H. Mack. 2000. How self-tolerance and the immunosuppressive drug FK506 prevent B-cell mitogenesis. *Nature*. 403:672–676.

Grumont, R.J., A. Strasser, and S. Gerondakis. 2002. B cell growth is controlled by phosphatidylinositol 3-kinase-dependent induction of Rel/NF-kappaB regulated c-myc transcription. *Mol. Cell*. 10:1283–1294.

Hardy, R.R., and K. Hayakawa. 2001. B cell development pathways. *Annu. Rev. Immunol.* 19:595–621.

Harris, A.W., C.A. Pinkert, M. Crawford, W.Y. Langdon, R.L. Brinster, and J.M. Adams. 1988. The Eμ-*myc* transgenic mouse. A model for high-incidence spontaneous lymphoma and leukemia of early B cells. *J. Exp. Med.* 167:353–371.

Hayashi, K., M. Yamamoto, T. Nojima, R. Goitsuka, and D. Kitamura. 2003. Distinct signaling requirements for Dmu selection, IgH allelic exclusion, pre-B cell transition, and tumor suppression in B cell progenitors. *Immunity*. 18:825–836.

Heim, R., T. Iwata, E. Zvaritch, H.P. Adamo, B. Rutishauser, E.E. Strehler, D. Guerini, and E. Carafoli. 1992. Expression, purification, and properties of the plasma membrane Ca2+ pump and of its N-terminally truncated 105-kDa fragment. *J. Biol. Chem.* 267:24476–24484.

Hendriks, R.W., and R. Kersseboom. 2005. Involvement of SLP-65 and Btk in tumor suppression and malignant transformation of pre-B cells. *Semin. Immunol*. 18:67–76.

Hendriks, R.W., and S. Middendorp. 2004. The pre-BCR checkpoint as a cell-autonomous proliferation switch. *Trends Immunol.* 25:249–256.

Im, S.H., and A. Rao. 2004. Activation and deactivation of gene expression by Ca2+/calcineurin-NFAT-mediated signaling. *Mol. Cells*. 18:1–9.

Iritani, B.M., K.A. Forbush, M.A. Farrar, and R.M. Perlmutter. 1997. Control of B cell development by Ras-mediated activation of Raf. *EMBO J.* 16:7019–7031.

Iritani, B.M., J. Alberola-Ila, K.A. Forbush, and R.M. Perimutter. 1999. Distinct signals mediate maturation and allelic exclusion in lymphocyte progenitors. *Immunity*. 10:713–722.

June, C.H., and P.S. Rabinovitch. 1990. Flow cytometric measurement of intracellular ionized calcium in single cells with indo-1 and fluo-3. *Methods Cell Biol.* 33:37–58.

Knoepfler, P.S., P.F. Cheng, and R.N. Eisenman. 2002. N-myc is essential during neurogenesis for the rapid expansion of progenitor cell populations and the inhibition of neuronal differentiation. *Genes Dev.* 16:2699–2712.

Langdon, W.Y., A.W. Harris, S. Cory, and J.M. Adams. 1986. The c-myc oncogene perturbs B lymphocyte development in E-mu-myc transgenic mice. *Cell*. 47:11–18.

Li, L.H., C. Nerlov, G. Prendergast, D. MacGregor, and E.B. Ziff. 1994. c-Myc represses transcription in vivo by a novel mechanism dependent on the initiator element and Myc box II. *EMBO J.* 13:4070–4079.

Morrow, M.A., G. Lee, S. Gillis, G.D. Yancopoulos, and F.W. Alt. 1992. Interleukin-7 induces N-myc and c-myc expression in normal precursor B lymphocytes. *Genes Dev.* 6:61–70.

Murphy, M.J., A. Wilson, and A. Trumpp. 2005. More than just proliferation: Myc function in stem cells. *Trends Cell Biol.* 15:128–137.

Pelengaris, S., M. Khan, and G. Evan. 2002. c-MYC: more than just a matter of life and death. *Nat. Rev. Cancer*. 2:764–776.

Rawlings, D.J. 1999. Bruton's tyrosine kinase controls a sustained calcium signal essential for B lineage development and function. *Clin. Immunol.* 91:243–253.

Rickert, R.C., J. Roes, and K. Rajewsky. 1997. B lymphocyte-specific, Cre-mediated mutagenesis in mice. *Nucleic Acids Res.* 25:1317–1318.

Sauer, B. 2002. Cre/lox: one more step in the taming of the genome. *Endocrine*. 19:221–228.

Shiio, Y., S. Donohoe, E.C. Yi, D.R. Goodlett, R. Aebersold, and R.N. Eisenman. 2002. Quantitative proteomic analysis of Myc oncoprotein function. *EMBO J.* 21:5088–5096.

Shinkai, Y., G. Rathbun, K.P. Lam, E.M. Oltz, V. Stewart, M. Mendelsohn, J. Charron, M. Datta, F. Young, A.M. Stall, et al. 1992. RAG-2-deficient mice lack mature lymphocytes owing to inability to initiate V(D)J rearrangement. *Cell*. 68:855–867.

Staller, P., K. Peukert, A. Kiermaier, J. Seoane, J. Lukas, H. Karsunky, T. Moroy, J. Bartek, J. Massague, F. Hanel, and M. Eilers. 2001. Repression of p15INK4b expression by Myc through association with Miz-1. *Nat. Cell Biol.* 3:392–399.

Thompson, C.B., E.H. Humphries, L.M. Carlson, C.L. Chen, and P.E. Neiman. 1987. The effect of alterations in myc gene expression on B cell development in the bursa of Fabricius. *Cell*. 51:371–381.

Webb, S.E., and A.L. Miller. 2003. Calcium signalling during embryonic development. *Nat. Rev. Mol. Cell Biol.* 4:539–551.

Wen, R., Y. Chen, J. Schuman, G. Fu, S. Yang, W. Zhang, D.K. Newman, and D. Wang. 2004. An important role of phospholipase Cgamma1 in pre-B-cell development and allelic exclusion. *EMBO J.* 23:4007–4017.

Whitfield, J.F. 1992. Calcium signals and cancer. *Crit. Rev. Oncog.* 3:55–90.

Winslow, M.M., E.M. Gallo, J.R. Neilson, and G.R. Crabtree. 2006. The calcineurin phosphatase complex modulates immunogenic B cell responses. *Immunity*. 24:141–152.

Zeller, K.I., X. Zhao, C.W. Lee, K.P. Chiu, F. Yao, J.T. Yustein, H.S. Ooi, Y.L. Orlov, A. Shahab, H.C. Yong, et al. 2006. Global mapping of c-Myc binding sites and target gene networks in human B cells. *Proc. Natl. Acad. Sci. USA*. 103:17834–17839.

Zimmerman, K., and F.W. Alt. 1990. Expression and function of myc family genes. *Crit. Rev. Oncog.* 2:75–95.